PARAMETRIC DYNAMICS OF QUANTUM SYSTEMS AND TRANSITIONS BETWEEN ENSEMBLES OF RANDOM MATRICES

KAROL ŻYCZKOWSKI

Instytut Fizyki, Uniwersytet Jagielloński
Reymonta 4, 30-059 Kraków, Poland

(Received January 7, 1993)

We analyze ensembles of random matrices capable of describing the transitions between orthogonal, unitary and Poisson ensembles. Scaling laws found in complex Hermitian band random matrices and in additive random matrices allow us to apply them to represent the changes of the statistical properties of quantum systems under a variation of external parameters. The properties of spectrum and eigenvectors of an illustrative dynamical system are compared with the properties of ensembles of random matrices. To describe the motion of the eigenvectors of the matrix representing a dynamical system under a change of external parameters we define the relative localization length of the eigenvectors and analyze its properties. We propose a criterion for selection of generic basis, in which statistics of eigenvector components might be described by random matrices. The properties of products of unitary matrices, representing composed quantum systems, are investigated.

PACS numbers: 05.45. +b, 02.50. +s, 24.60. Ky

1. Introduction

The properties of quantum analogues of classically chaotic systems have attracted the attention of physicists for over a decade. In the pioneering work of Casati *et al.* [1] it was shown, on the basis of a numerical analysis of the kicked rotator, that quantum effects limit the diffusion in the momentum space characteristic of classically chaotic systems. This observation led to a thorough investigation of analogues of other classically chaotic systems and several similarities and differences between the properties of classical and corresponding quantum systems have been revealed (see [2–4] and references therein). The term *chaos* has a precise definition in classical mechanics based on the divergence of neighbouring trajectories in phase space [5, 6]

and the positiveness of the Lapunov exponent. Since the concept of a single trajectory loses its meaning in quantum mechanics a generalization of the definition of chaos for quantum systems is not simple. Some efforts in this direction have been only partially successful [7–10]. One usually applies, therefore, a phenomenological method, analyzing various properties of quantum systems [4, 11, 12] the classical analogues of which display chaotic behaviour.

Numerous studies of chaotic quantized systems have shown [11–15] that the statistical properties of the spectra and eigenstates of dynamical systems are well described by ensembles of random matrices. The theory of random matrices was developed by Wigner, Porter and Mehta in order to explain the complicated structure of compound nuclei [16–18]. In spite of a lack of a precise proof, it is known [11] which ensembles of random matrices correspond to a given quantum dynamical system. Time independent, autonomous systems are described by Hermitian matrices of Gaussian ensembles (GE) [17, 18], while time dependent, periodically driven systems are characterized by unitary matrices of circular Dyson ensembles (CE) [18, 19]. For both categories one of three universal ensembles is appropriate depending on the symmetry of the system: the orthogonal ensembles (GOE and COE) describe systems with an antiunitary symmetry (generalized time-reversal symmetry) while the unitary ensembles (GUE and CUE) characterize systems without such symmetry [11, 20]. The third class, the symplectic ensembles (GSE and CSE), correspond to systems where so-called Kramers' degeneracy occurs (half integer spin and exactly one antiunitary symmetry) [11, 21].

It is worth emphasizing an essential difference in the search for chaos in classical and quantum systems. Studying classical dynamics we analyze the time evolution of the system to find the sign of the largest Lapunov exponent. On the other hand in quantum mechanics a relevant piece of information might be extracted by studying the properties of the stationary solutions of the corresponding Schrödinger equation. A complementary approach based on the investigation of the time evolution of wave packets in quantum models was developed only recently [22].

Simple statistical measures of the spectrum (level spacing distribution $P(s)$) have universal properties and are the same for various quantum systems with the same symmetry properties [20]. On the other hand, an investigation of the long-range correlation of the spectra measured by the number variance $\Sigma^2(L)$ or the spectral rigidity $\Delta_3(L)$ displays for larger values of L some relevant deviations from the predictions of the random matrix theory. These differences are found [23] to be system specific and are linked to the existence of periodic orbits in classical phase space [24].

Recent years have brought a deeper understanding of the fundamen-

tal concepts of quantization of classically chaotic systems. The Gutzwiller theory of periodic orbits [25, 26] has made it possible to find a semiclassical approximation for the smoothed level density in a quantum spectrum [27–30]. The Einstein–Brillouin–Keller (EBK) quantization conditions are suitable for integrable systems only [31, 32]. Quantization conditions applicable to classically chaotic systems based on the periodic orbits have been found [33–36]. The wave packet propagation technique was proposed and further developed by Heller [22, 37]; other semiclassical methods of quantization are based on an adiabatically switched perturbation [38–42] or on building an approximate integrable Hamiltonian [43, 42]. In spite of these considerable achievements several problems of the semiclassical quantization of classically chaotic systems remain unsolved (see [42] and references therein) and the field still offers a challenge for theoretical physicists.

The study of quantum chaotic systems, sometimes called *quantum chaology* [44, 45], is of great interest not only from the theoretical point of view. Recent experiments on the microwave ionization of Rydberg atoms [46–50] and on the structure of hydrogen atoms in a strong magnetic field [51–56] have shown the connections between quantum chaology and atomic physics. The problems of quantum chaos are present in the theory of nuclear structure and nuclear reactions (see [57, 58] and references therein), Ericson fluctuations [59, 60] and chaotic scattering [61–64]. Quantum chaology is also linked to solid state physics *via* the phenomenon of Anderson localization in disordered media [65, 66] and the theory of conductance fluctuations [67–69]. The recent investigation of absorption spectra in microwave resonators [70–72] provided an interesting possibility for a complementary experimental verification of theoretical predictions concerning the properties of quantized billiards. The eigenfrequencies of a resonator in the shape of the Sinai billiard display level repulsion [70], a characteristic to quantum chaotic systems [73, 13] and GOE matrices [18]. The probability of finding clustered eigenfrequencies is larger for a rectangular resonator [72] and the spacing statistics is closer to the Poisson distribution typical of classically regular systems [74, 11].

The transition from regular motion to chaos in classical systems is well understood [6, 12, 75]. Consider an integrable system, described by a Hamiltonian $\widehat{A}_0$, and the perturbed system

$$\widehat{A} = \widehat{A}_0 + \lambda \widehat{V} . \tag{1}$$

The Kolomogorov–Arnold–Moser (KAM) theorem states that for small, but non-zero values of the control parameter λ, the nonintegrable system $\widehat{A}$ is non-chaotic [76–78]. Only if the perturbation strength exceeds a critical value λ_c are the last KAM tori broken and full scale chaos occurs [6, 79]. A rough estimate of the critical parameter value is provided by the Chirikov

resonance overlap criterion [80]. More accurate results might be obtained applying the renormalization technique [82–84]. In spite of considerable efforts, attempts to generalize the KAM theorem for quantum mechanics have been only partially successful [84, 85] but the role played in quantum models by analogues of the classical KAM tori is well established [86, 87].

The changes of the properties of a quantum system with the perturbation parameter λ may be well described by a novel method called *level dynamics*, introduced by Pechukas [88]. In this approach, eigenvalues of the quantum system are considered as a set of interacting classical particles, while the parameter λ plays the role of a fictitious time. Changes of eigenvalues with the control parameter are regarded as the dynamics of the classical system consisting of point particles [89–92, 11]. It has been shown that such a dynamical system is integrable and a sufficient number of integrals of motion exist. The level dynamics of an autonomous quantum system corresponds to the generalized Calogero–Moser system [93] of classical particles moving in one-dimensional unbounded space [94]. A periodically driven quantum system is described by a unitary Floquet operator with eigenphases moving along the unit circle. In this case the level dynamics leads to the integrable Sutherland model [95]. Integrability of the level dynamics means that knowing the initial conditions of the particles for $\lambda = 0$ (the eigenvalues of the unperturbed system), one may get the position of the interacting particles (hence the eigenvalues of the quantum system) for an arbitrary value of the fictitious time λ. Moreover, it is known [96] that the thermodynamic equilibrium of the interacting particles moving along the unitary circle corresponds to the state of a quantum system described by the circular unitary ensemble of random matrices.

In order to measure to correlations between the spectra of quantum systems obtained for different values of the system parameters, the parametric number variance has been introduced [97]. Complementary information on the level dynamics may be obtained by studying the distribution of curvatures [98–101], defined by the second derivative of the energy levels with respect to the perturbation parameter. The curvature distributions for all three universality classes are known [102]. Investigation of avoided crossings between adjacent levels provides an additional possibility for characterizing the level dynamics [103]. Distribution of the minimal distances of avoided crossings [104–106] or the related distribution of the exceptional points [107] allows us to distinguish between different universality classes or to study the transitions between them [108, 109].

In order to investigate the motion of energy levels under the changes of parameters, we may use autonomous quantum systems such as the hydrogen atom in an uniform magnetic field of varying strength [97, 105] and quantum billiards with varying geometry [97, 99, 101] or periodically driven

model systems such as the kicked top [100, 108] and kicked rotator [101]. Complementary investigations have been carried out directly with random matrices representing the Hamiltonian (1) [20, 98, 102]. In order to analyze the level dynamics of a fictitious quantum system one may take the matrices A_0 and V from the same ensemble and vary values of the parameter λ. On the other hand, taking the matrices A_0 and V from different ensembles one can study the transitions between them [11, 20].

The set of three universal ensembles (orthogonal, unitary and symplectic) describing quantum chaotic systems might be enlarged by defining a fourth class of diagonal matrices containing real random numbers generated according to a Gaussian distribution. Such matrices give (in the limit of large matrix size N) the Poisson distribution of eigenvalues and are therefore suitable for representing quantum analogues of classically regular systems [11]. By taking the matrix A_0 from this ensemble and the matrix V from GOE we may construct an additive model of random matrices describing the transition between Poisson and orthogonal ensembles [110–113]. The scaling properties of this ensemble have been demonstrated [114]: the statistical properties of the spectrum of random matrices depend only on a scaled perturbation parameter $\tilde{\lambda} = \lambda\sqrt{N}$. In this way the additive model of random matrices provides a family of level spacing distributions interpolating between the Poisson and GOE distributions and labeled by the scaled parameter $\tilde{\lambda}$. The explicit form of this distribution is not known, but the formula obtained for 2×2 matrices gives a reasonable approximation useful for fitting to numerical data [113, 114].

Another ensemble of random matrices interpolating between the Poisson and GOE consists of $N \times N$ matrices with non-zero elements inside a band of width b [115]. Each element is drawn independently according to Gaussian distribution with zero mean and the variance dependent on N and b [116]. By varying the width b of the band from 1 to N one can study the transition between Poisson and Gaussian orthogonal ensembles [115–118]. The band random matrices also possess a scaling property: the statistical properties of the eigenvalues [116–118] and eigenvectors [119, 120] depend on the single variable $x = b^2/N$. A fair approximation to the level spacing distribution $P_x(s)$ was recently proposed [4, 118]. This distribution has been found to be useful for describing the properties of the quantum dynamical systems represented by matrices with a band-like structure, *e.g.* the quantum kicked rotator [1, 4, 121].

Apart from the families of distributions originating from ensembles of random matrices (additive matrices [113], band matrices [118, 122]), there exist several other distributions interpolating between the Poisson and GOE level spacing distributions. A simple formula proposed by Brody [16, 17] is based on the assumption that for small spacings s the levels repel each

other as $P(s) \sim s^q$, where the parameter q varies from zero to unity. In spite of lack of precise physical arguments supporting this hypothesis the Brody distribution seems to have had the greatest success in fitting experimental and numerical data [4, 123]. Furthermore, its generalization [124] has been used to develop an approximation of the distribution $P_x(s)$ characteristic of band random matrices [118]. Another family of interpolating distributions is due to Berry and Robnik [125], who have proposed to perform a convolution of Poisson and Wigner distributions. Theirs distribution is parametrized by a relative weight $r \in (0, 1)$ proportional to the fraction of the phase space of the corresponding classical system occupied by the regular islands of stable motion. Some other similar distributions have been proposed [4, 123–127] but it is not at all known to what dynamical quantum systems they apply. Moreover, it is not clear, which properties of quantum systems with varying parameters are universal and which are system dependent.

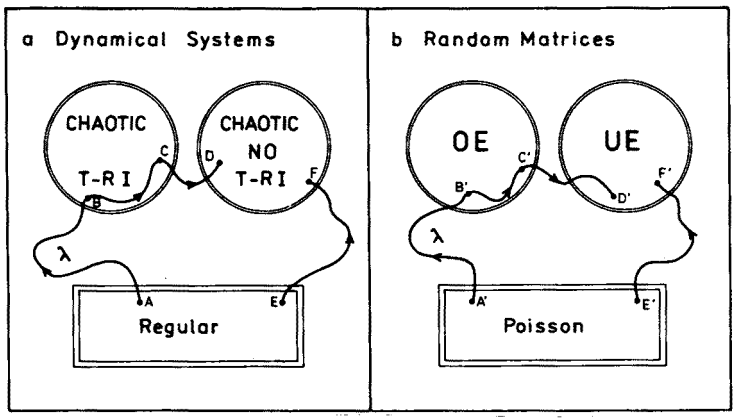

Fig. 1. Sketch of the transitions in the space of: a) quantum dynamical systems; b) random matrices. For further explanations see the text.

In this work we continue the investigation of the link between the parametric changes of quantum dynamical systems and transitions in the space of random matrices. In particular, we investigate the dynamics of eigenbasis of a quantum system under a change of external parameters. Fig. 1.a is a schematic representation of the space of quantum dynamical systems. The lower rectangle symbolizes the analogues of classically regular systems. The two circles above stand for the subsets of classically chaotic systems with and without time-reversal symmetry. Note that the borders of these sets, represented by sharp lines in the picture, should be rather diffuse, since the transition to/from chaos in classical systems often occurs in a continuous way [5, 6]. Each of the points A, B, C, D, E, F in the picture represents a single quantum system, while the paths connecting them stand for trajectories in the space of dynamical systems or the level dynamics with respect

to the change of a parameter λ.

The right part of the figure represents the space of random matrices: the lower rectangle stands for the diagonal matrices of a Poisson ensemble, the circles above it for the orthogonal and unitary ensembles. Points A', B', C', D', E', F' represent single matrices and lines joining them represent the transition between random matrices, or more generally, between ensembles of random matrices. Further on we will be concerned with two basic questions: *(i)*. Which transitions in the space of dynamical systems possess some universal features?, and *(ii)*. To what extend are we able to find a one-to-one correspondence between the transition in the space of dynamical systems and the transitions between random matrices?

In fact, one could imagine the two pairs of pictures: one symbolizing on the left hand side the space of autonomous dynamical quantum systems and on the right hand side the space of Hermitian random matrices (Gaussian ensembles). The other pair would portray the space of periodically driven quantum systems and the space of unitary random matrices (circular ensembles). Note that to simplify the above schematic diagram we have not taken into account quantum systems with the Kramers' degeneracy [11] and the matrices pertaining to the symplectic ensemble.

This paper is organized as follows. Section 2 is concerned with random matrices. In the first subsection we present a brief review of the properties of classical ensembles of random matrices. In the next subsection we study the additive model of random matrices in more detail, analyzing how the eigenvectors of a matrix change with the variation of the parameter λ. In order to measure these changes in a quantitative way we introduce the relative mean entropy of the eigenvectors and the relative localization length. Band random matrices are discussed in the following subsection. We define and analyze an ensemble of complex Hermitian band random matrices capable of describing transitions between Poisson, Gaussian orthogonal and Gaussian unitary ensembles. Defining the generalized localization length of eigenvectors, we demonstrate the scaling features of this model.

In Section 3 the statistical properties of quantum-dynamical systems are discussed. The first subsection is concerned with eigenvalues, the next with eigenvectors and the last with level dynamics. In Section 4 we analyze an example of dynamical system: the model of a periodically kicked top [15, 128–131]. The first subsection is concerned with some properties of the classical model. In the next, we compare the behaviour of the quantum model under variation of the parameters of the system and transitions between Poisson and orthogonal ensembles of random matrices. The level spacing distribution, the eigenvector statistics and the mean entropy during the transition are discussed. We analyze the distribution of eigenvectors represented in a basis generated from the eigenbasis of the system by a

generalized rotation. Moreover, we provide a simple criterion for selection of generic basis, in which eigenvector statistics might be described by the canonical ensembles of random matrices.

In the next subsection the transition between the orthogonal and unitary ensembles is analyzed. In particular, we link this transition with the breaking of time reversal symmetry in the corresponding classical model and extend the results obtained previously in references [132–134]. The properties of products of unitary matrices, which correspond to composed, periodical quantum systems are investigated. We conclude in Section 5 by summarizing our results and presenting a list of open questions.

2. Random matrices

2.1. Canonical ensembles: orthogonal, unitary and symplectic

There exist three Gaussian ensembles of matrices studied by Mehta [16, 18] (GOE, GUE and GSE), which are invariant under orthogonal, unitary and symplectic transformations, respectively. They are closely related to three circular ensembles of unitary matrices (COE, CUE, CSE) introduced later by Dyson [19]. The density of quasi energy eigenphases of all three circular ensembles is uniform in the interval $(0, 2\pi)$, while the density of eigenvalues of the Hermitian matrices pertaining to any of the Gaussian ensembles is given by the famous semicircle law of Wigner [16]. In order to study the statistical properties of the spectrum in this case the technique of spectral unfolding is needed [135, 20], which compensates the changes of the density with energy. Interestingly, the theory of random matrices predicts the same statistics of eigenvalues and eigenvectors for the corresponding Gaussian and circular ensembles [17, 18].

The nearest level spacing distribution $P(S)$, often used to characterize spectral fluctuations, is well approximated by the so-called Wigner surmise:

$$P_1(S) = \frac{\pi}{2} S \exp\left[-\frac{\pi S^2}{4}\right], \tag{2}$$

$$P_2(S) = \frac{32}{\pi^2} S^2 \exp\left[-\frac{4S^2}{\pi}\right], \tag{3}$$

$$P_4(S) = \left(\frac{64}{9\pi}\right)^3 S^4 \exp\left[-\frac{64S^2}{9\pi}\right], \tag{4}$$

for the orthogonal, unitary and symplectic ensembles, respectively [17]. It is worth noting that other measures of the statistical properties of the spectrum, like the two point correlation function $R_2(S)$, the spectral rigidity $\Delta_3(L)$ and the number variance $\Sigma^2(L)$ also have identical forms for both

the families of Gaussian and circular ensembles (in the limit of large matrix size N) [18].

Relevant information on the ensemble of random matrices is carried not only by spectra of matrices, but also, independently, by their eigenvectors [16]. Numerical diagonalization of a matrix provides N eigenvectors $|\psi_k\rangle, k = 1, \ldots, N$, each described by N components $c_k^l, l = 1, \ldots, N$. The eigenvectors are represented in the basis, in which the random matrix is constructed. We are interested in the distribution of squared components $y_k^l = |c_k^l|^2$. To simplify the notation, we shall omit the indices labeling each squared component y. In the limit of large matrices the distribution of the squared moduli of components $P(y)$, called *eigenvector statistics*, is given for both kinds of ensembles by the same chi-square distribution [17, 136]

$$P_\beta(y) = \frac{(\beta/2)^{\beta/2}}{\Gamma(\beta/2)\langle y\rangle}\left(\frac{y}{\langle y\rangle}\right)^{\beta/2-1}\exp\left[-\frac{\beta y}{2\langle y\rangle}\right], \tag{5}$$

where the number of degrees of freedom β is equal to 1, 2 and 4 for OE, UE and SE, respectively, and $\langle y\rangle$ denotes the mean value of the eigenvector component. For the orthogonal ensemble ($\beta = 1$) this formula reduces to the Porter–Thomas distribution [16]

$$P(y) = \frac{1}{\sqrt{2\pi\langle y\rangle}}\exp\left(-\frac{y}{2\langle y\rangle}\right). \tag{6}$$

A single eigenvector of a random matrix ψ_k might be characterized by the Shannon entropy H_k [115]

$$H_k = -\sum_{l=1}^{N} y_k^l \ln(y_k^l). \tag{7}$$

This quantity varies from zero for a totally localized eigenvector (one component equal to unity and all others to zero) to $\ln(N)$ for a delocalized eigenvector with all components equal to $1/N$. The entire matrix A is characterized by the mean entropy

$$\langle H\rangle = \frac{1}{N}\sum_{k=1}^{N} H_k. \tag{8}$$

For random matrices representing a member of a canonical ensemble the mean information entropy can be found analytically [137] and expressed by means of the Digamma Function Ψ [138]

$$\bar{H}_\beta = \Psi\left(\frac{\beta N}{2}+1\right) - \Psi\left(\frac{\beta}{2}+1\right), \tag{9}$$

with $\beta = 1, 2$ and 4 for OE, UE and SE, respectively.

A matrix pertaining to the Gaussian orthogonal ensemble might be easily constructed on a computer by means of a generator of pseudo-random numbers. It is a real, symmetric matrix with elements generated independently according to a Gaussian distribution with zero mean and the variance $\sigma_{ij}^2 = (1 + \delta_{ij})/N$ [17]. A schematic diagram of such a matrix is depicted in Fig. 2.b.

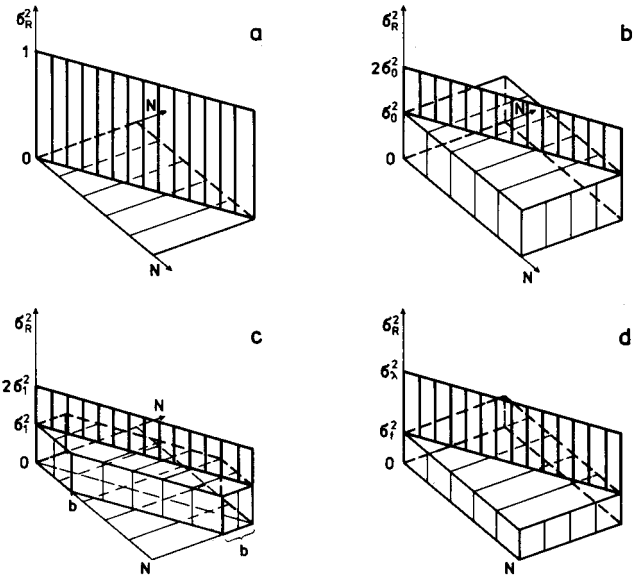

Fig. 2. Scheme of the random matrices: a) Poisson, b) GOE, c) band matrices, d) additive model. Real symmetric matrices consist of random numbers generated according to a Gaussian distribution with zero mean and variance σ^2, as depicted for each element of the $N \times N$ matrix.

The Gaussian unitary ensemble consists of complex Hermitian matrices. The real and imaginary parts of each element are generated independently according to a Gaussian distribution with zero mean and the variance $(\sigma_{ij}^R)^2 = (1 + \delta_{ij})/2N$ and $(\sigma_{ij}^I)^2 = (1 - \delta_{ij})/2N$, respectively [17]. The Gaussian symplectic ensemble contains real quaternion matrices of dimension $2N \times 2N$. They might be decomposed [18] into a sum of four terms $A = A_0\varepsilon_0 + A_1\varepsilon_1 + A_2\varepsilon_2 + A_3\varepsilon_3$, where ε_i; $i = 0, 1, 2, 3$ are the Pauli matrices, A_0 is a real $N \times N$ symmetric matrix, A_j; $j = 1, 2, 3$ are real $N \times N$ antisymmetric matrices and $A_j\varepsilon_i$ stands for the tensor product [18].

As a fourth universality class, one can consider the diagonal matrices of real random elements in the case of Gaussian ensembles (or the unitary matrices with random eigenphases in the case of circular ensembles). Both

ensembles display Poisson statistics in their spectra

$$P(s) = e^{-s} \tag{10}$$

and are appropriate to for the description of classically regular systems [11]. The scheme of a matrix representing the Gaussian Poisson ensemble is shown in Fig. 2.a.

2.2. Interpolating ensembles: additive model

Simplest ensembles of matrices interpolating in a continuous way between the canonical Gaussian ensembles may be based on assumption (1). In order to keep the eigenvalues of the matrix A in a bounded range of the energy axis it is convenient to modify [113, 114] equation (1):

$$A = \frac{A_0 + \lambda V}{\sqrt{1+\lambda^2}}. \tag{11}$$

Taking for A_0 the diagonal random matrices and for V the members of the Gaussian orthogonal ensemble we define an ensemble of random matrices interpolating between Poisson ensemble and GOE. A scheme of such an additive random matrix is shown in Fig. 2.d. The diagonal real elements of the matrix are taken with a Gaussian distribution with zero mean and variance σ_λ^2 set to [113]

$$\sigma_\lambda^2 = \frac{1}{1+\lambda^2}\left(1 + \frac{2\lambda^2}{N}\right). \tag{12}$$

The variance characterizing the off-diagonal elements reads

$$\sigma_f^2 = \frac{\lambda^2}{N(1+\lambda^2)}. \tag{13}$$

Note that the above variances are determined up to an irrelevant scale factor, which settles the radius of the semicircle distribution of the level density in the limiting case of an orthogonal ensemble [17]. Increasing the value of the parameter λ from zero to infinity, one may study the transition from Poisson to GOE, represented schematically in Fig. 1.b by the path $A' - B'$ in the space of random matrices.

Motivated by a possible application to the description of the semiclassical regime of quantum dynamical systems we are interested in large random matrices defined by equation (11). In this case we are unlikely to get an analytical expression for the joint distribution function of eigenvalues or the level spacing distribution in a general case [20]. However, it is possible to

obtain analytical results for the model of 2×2 random matrices. For the case of the transition Poisson — GOE the level spacing distribution P(s) may be expressed [113, 114] in terms of a modified Bessel function $I_0(x)$ and a Tricomi function [138, 139] $U(a, b, x)$ as:

$$P_\lambda^{PO}(s) = \left(s\frac{u(\lambda)^2}{\lambda}\right) \exp\left(-\frac{u(\lambda)^2}{4\lambda^2}s^2\right) \int_0^\infty \mathrm{e}^{(-x^2-2x\lambda)} I_0\left(\frac{sx}{\lambda}u(\lambda)\right) dx\,, \tag{14}$$

where $u(\lambda) = \sqrt{\pi}U(-1/2, 0, \lambda^2)$. The above distribution reduces to Poisson e^{-s} for $\lambda = 0$, while the Wigner surmise (2) is approached in the limit $\lambda \to \infty$. For all intermediate values of λ, the distribution (14) exhibits an linear repulsion of eigenvalues, *i.e.* $P_\lambda(s) \sim s/\lambda$, for $s < \lambda \ll 1$. This distribution was shown to be useful for describing the spectral properties of large random matrices [114]. The best fit of the distribution (12) to the numerical data obtained from random matrices delivers the fitting value λ_f. A detailed investigation has shown that the transition speed differs from one part of the spectrum to the other, so the best fit parameter λ_f is different for a group of eigenvalues taken from the wings of the spectrum and for a group of eigenvalues taken from its center. Taking this fact into account and analyzing each part of the spectrum independently, a scaling relation has been found [114], $\lambda_f = \lambda_f(\bar{\lambda})$, where the scaling parameter $\bar{\lambda}$ is equal

$$\bar{\lambda} = \sqrt{N}\lambda\,. \tag{15}$$

Because of the above scaling relation the additive model of random matrices might be used to describe the behaviour of dynamical systems. A possible application to quantized, pseudointegrable systems was recently proposed [72, 140, 141].

In a similar manner, by taking for V the complex random matrices pertaining to the unitary ensemble, one can study the transition Poisson — GUE. The level spacing distribution obtained for the 2×2 complex matrices in the case of this transition reads [142]

$$P_\lambda^{PU}(s) = s\sqrt{\frac{2}{\pi}}\frac{a^2}{\lambda} \exp\left[-\frac{a^2}{2\lambda^2}s^2\right] \int_0^\infty \sinh\left[\frac{sxa}{\lambda}\right] \frac{\exp\left[-\lambda x - \frac{x^2}{2}\right]}{x} dx\,, \tag{16}$$

where the coefficient $a(\lambda)$ is expressed by the error function $\mathrm{erf}(x)$, the exponential integral $\mathrm{Ei}(x)$ and a hypergeometric function ${}_2F_2(a, b, c; z)$ [138, 139]

$$a(\lambda) = \sqrt{\frac{2}{\pi}}\lambda + \left(1 - \mathrm{erf}\left(\frac{\lambda}{\sqrt{2}}\right)\right) \exp\left(\frac{\lambda^2}{2}\right)$$

$$-\lambda^2\left[\frac{\mathrm{Ei}\left(\frac{\lambda^2}{2}\right)}{2}+\sqrt{\frac{2}{\pi}}\lambda_2 F_2(1/2,3/2,3/2;\lambda^2/2)\right]. \quad (17)$$

Formula (16) reduces to the Poisson distribution for $\lambda = 0$ and the Wigner surmise (3) with quadratic level repulsion, characteristic to the unitary ensemble, is obtained in the limit $\lambda \to \infty$. In Fig. 1.b this transition is represented by the path $E' - F'$.

The additive model (11) is also useful for studying the transition GOE–GUE. The level spacing distribution obtained for 2×2 matrices reads [142–145]

$$P_\lambda^{OU}(s) = s\sqrt{\frac{2+\lambda^2}{2}}a^2 \exp\left[-\frac{s^2a^2}{2}\right]\mathrm{erf}\left[\frac{sa}{\lambda}\right], \quad (18)$$

where

$$a(\lambda) = \sqrt{\frac{\pi(2+\lambda^2)}{4}}\left[1-\frac{2}{\pi}\left[\arctan\left(\frac{\lambda}{\sqrt{2}}\right)-\frac{\sqrt{2}\lambda}{2+\lambda^2}\right]\right]. \quad (19)$$

This distribution, being a generalization of the Favro–McDonald formula [146], reduces to the equation (2) for $\lambda = 0$ and to the equation (3) in the limit $\lambda \to \infty$. The above distribution obtained for the 2×2 matrices was found to be applicable to the description of statistical properties of large matrices interpolating between orthogonal and unitary ensembles [143]. The transition between orthogonal and unitary ensembles is of great physical interest, since it corresponds to the breaking of a generalized antiunitary symmetry in a dynamical system. The influence of time reversal symmetry breaking for the statistical properties of the spectrum was first observed in nuclear physics [16]. Similar results were obtained by analyses of the conductance fluctuations of mesoscopic systems in an external magnetic field [60, 67, 68]. In addition the OE–UE transition has been studied for model dynamical systems like billiards in a magnetic field [147], Aharonov–Bohm billiards, the coupled spin system [148], or the periodically kicked top [134, 143].

The additive model (1) might also be used to study the level dynamics inside a given ensemble. For example, by taking both matrices A_0 and V in equation (11) from the orthogonal ensemble, we may mimic the parametric dynamics of classically chaotic dynamical systems, represented in figure 1a by the path $B - C$. This method was used to find universal distributions of curvatures for parametric motion in the orthogonal, unitary and symplectic ensembles [98]. Similar results were obtained by studying an alternative level dynamics defined by [102],

$$A = A_0 \cos(\tau) + V \sin(\tau), \quad (20)$$

where both matrices belong to the same ensemble. A suitable substitution $\lambda = \tan(\tau)$ shows that equations (20) and (11) are equivalent. Note that in this model all eigenvalues are restricted to a certain energy interval, or speaking in the language of level dynamics, the "gas of particles" is confined [11].

The eigenvector statistics of the additive random matrices interpolating between Poisson and GOE was studied in reference [114] and an approximate formula, based on 2×2 matrices, was proposed

$$P(y) = \frac{2\lambda\sqrt{4+\lambda^2}}{\sqrt{y}\pi(\lambda^2 + 4y(4+\lambda^2))}\alpha\,. \tag{21}$$

The factor $\alpha = (N-1)/N$ takes into account the fact that the diagonal elements of the diagonalizing matrix are excluded. For small values of the perturbation parameter λ this formula has been shown [114] to be useful for describing the eigenvector statistics of arbitrary large matrices. In contrast to the scaling properties of the spectrum (14), the eigenvector statistics of the additive model does not depend on the matrix size N, at least for small values of the parameter λ.

The eigenvector statistics depends, in an obvious manner, on the basis in which the eigenvectors are expanded. In the case of additive random matrices it is natural to use the basis in which the matrix itself is constructed (*i.e.* the eigenbasis of the matrix obtained with $\lambda = 0$). On the other hand, one may also apply for this purpose any other orthogonal basis $\{|\varphi_i\rangle, i = 1, \ldots, N\}$. In this case the components of eigenvectors are equal $y = |\langle\psi_k(\lambda)|\varphi_i\rangle|^2$, and the explicit dependence of the eigenvectors $\{|\psi_k\rangle\}$ on the parameter λ is displayed. It is instructive to chose the basis $\{|\varphi\rangle\}$ as the eigenbasis of the matrix $A(\lambda + \Delta\lambda)$ and consider the distribution $P_{\Delta\lambda}(y)$ of components of the "rotated" eigenvectors

$$y = |\langle\psi_k(\lambda)|\psi_i(\lambda + \Delta\lambda)\rangle|^2\,. \tag{22}$$

The above defined statistics of rotated eigenvector components $P_{\Delta\lambda}(y)$ becomes singular for $\Delta\lambda \to 0$, but it is interesting to observe, how it depends on the rotation parameter $\Delta\lambda$. Denoting $\lambda_2 = \lambda_1 + \Delta\lambda$, we will also use an alternative notation for the statistics of rotated eigenvector components $P_{\lambda_1,\lambda_2}(y)$. In this notation the distribution is symmetric with respect to the change of the parameters, $P_{\lambda_1,\lambda_2}(y) = P_{\lambda_2\lambda_1}(y)$, and singular for $\lambda_1 = \lambda_2$. The distribution $P_{0,\lambda}(y)$ may thus symbolize the eigenvector statistics of the additive model $A \sim A_0 + \lambda V$ in the standard basis used to construct the matrix itself.

Figure 3 presents the eigenvector statistics for the additive model of random matrices. In order to make the differences between various distributions $P(y)$ more visible we use a logarithmic scale for the component y.

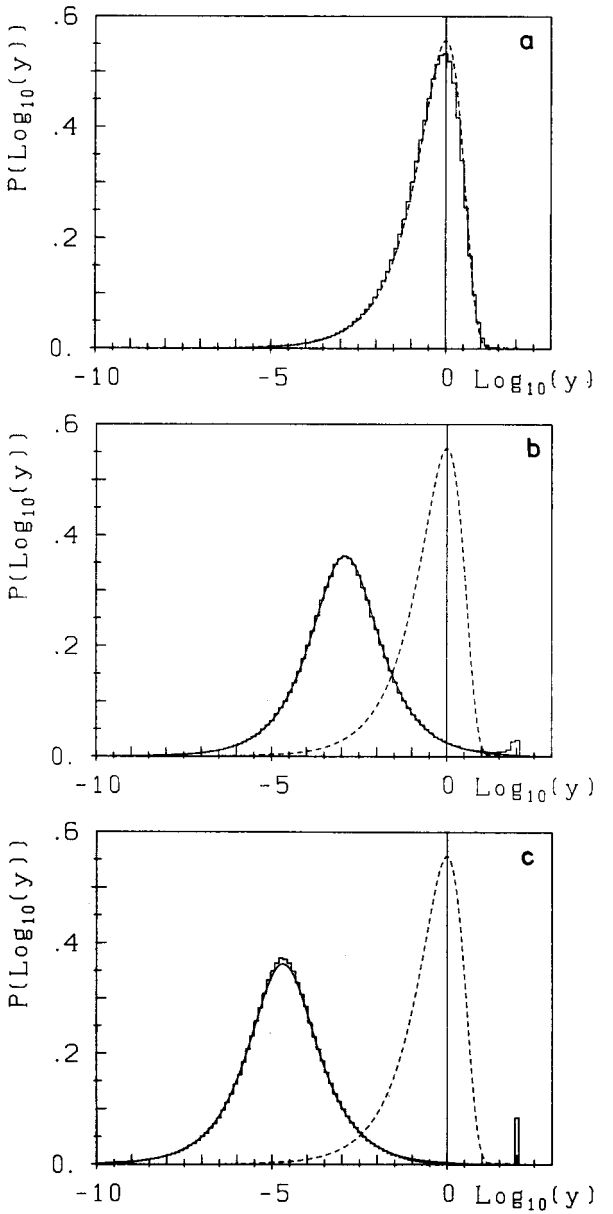

Fig. 3. Eigenvector statistics for the additive model of random matrices obtained for 200 matrices of size 100. a) "chaotic" case — statistics $P_{5.0,0.0}(y)$ well described by Porter–Thomas distribution; b) "regular" case — $P_{0.1,0.0}(y)$ and the distribution (21); c) "chaotic" case and rotated basis $P_{5.0,4.9}(y)$.

The normalization $\langle y \rangle = 1$ enables an easier comparison of the statistics obtained for matrices of different size N. Figure 3.a is obtained for $\lambda = 5.0$.

For such values of the perturbation parameter λ, the matrix A has the properties of GOE and the eigenvector statistics is well approximated by the Porter–Thomas distribution (7), denoted by the dashed line in the picture.

For small values of the perturbation parameter, only one component of each eigenvector is of the order of unity, while all others are some orders of magnitude smaller and are responsible for a dominant peak of the distribution $P(y)$ located at [114] $y_m \sim 2\log_{10}(\lambda) - 1$. Such a case is displayed in Fig. 3.b, obtained for a sample of 200 random matrices of size $N = 100$ with perturbation parameter $\lambda = 0.1$. The solid line stands for the distribution (21), drawn for the same value of λ without any fitting parameters. Note a small peak at $\log_{10}(y) \sim 2 = \log_{10}(N)$, which corresponds to a group of "diagonal" eigenvector components of the order of unity.

The significant difference between the two figures may provoke one to claim that the shape of the distribution $P(y)$, characterizing the additive random matrices, can be used as an absolute criterion for the GOE properties. This is not the case, as is demonstrated in Figure 3c. The probability distribution depicted here is obtained for the same value of the parameter $\lambda = 5.0$ as in Fig. 3.a. The only difference between these two cases lies in a rotation of the basis: Fig. 3.a presents the distribution $P_{5.0,0.0}(y)$ while Fig. 3.c shows the distribution $P_{5.0,4.9}(y)$. Observe that the latter distribution, obtained for matrix A close to the GOE regime, is quite similar to the similar to the one depicted in Fig. 3.b for a small value of the perturbation parameter λ. Best fit of the distribution (21) gives in this case the value $\lambda_f = 0.013$. A similar effect has also been observed for the eigenvector statistics of a matrix A_0 taken from the GOE and analyzed in the eigenbasis of $A = A_0 + \lambda A_1$, for a GOE matrix A_1 and small values of the parameter λ. In other words, the eigenvector statistics of a GOE matrix A, describing quantum chaotic systems, in a "wrong" basis (being to close to the eigenbasis of A) may look like the eigenvector statistics of a matrix with a Poisson level distribution, characteristic of classically regular systems. In the following sections of this work we discuss further the problem, in which basis is it "appropriate" to study the eigenvector statistics of a quantum dynamical system?

The distribution of components of rotated eigenvectors $P_{\Delta\lambda}(y)$ might be characterized by the mean entropy of eigenvectors $\langle H_\Delta \rangle$, defined in analogy to equations (7) and (8). Let us measure the entropy of rotated eigenvectors $\langle H_\Delta \rangle$ with respect to the mean entropy of eigenvectors of the orthogonal ensemble $\bar{H}_1$ given by (9) and introduce the relative entropy $\gamma = \langle H_\Delta \rangle / \bar{H}_1$. Figure 4 presents the dependence γ on $\Delta\lambda$ drawn in a log-log scale for two values of the matrix size N and the parameter λ_1. Standard method of the perturbation analyses gives a simple relation $\gamma \sim (\Delta\lambda)^2$. This behaviour

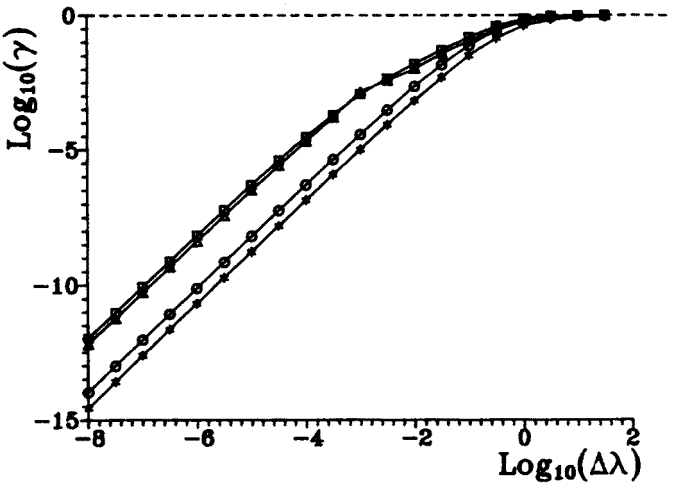

Fig. 4. Relative entropy of eigenvectors for the additive model of random matrices, depicted against the rotation parameter $\Delta\lambda$ for a) Poisson-like case $\lambda_1 = 0.001$ with $N = 100$ (□), $N = 10$ (△); b) Wigner-like case $\lambda_1 = 1.0$ with $N = 100$ (○), $N = 10$ (∗).

is visible in the picture for small values of the rotation parameter $\Delta\lambda$. For larger values of $\Delta\lambda$ the perturbation approach breaks down and differences between the cases of Poisson matrices ($\lambda_1 \ll 1$) and GOE–like matrices ($\lambda_1 > 1$) are clear. Independently of the value λ_1, characterizing the matrix A, for large enough values of the parameter λ_2, describing the basis in which the eigenvector statistics is calculated, the entropy of eigenvectors of the matrix A tends to the value typical to GOE. The size of the matrix N influences slightly the value of the entropy γ of eigenvectors, and consequently determines the magnitude of the rotation parameter $\Delta\lambda$ needed to produce delocalized eigenvectors.

2.3. Interpolating ensembles: band matrices

Hamiltonians of such quantum dynamical systems as atom in magnetic field [54–56], atom in microwave field [49, 50], the kicked top [1, 121, 149], kicked oscillator [150], and quantum bouncer [151, 152] are represented by matrices with a band like structure. This observation stimulated a search for an ensemble of band random matrices capable of describing the transition between Poisson and orthogonal ensembles [115–117]. Note that controlling the character of the random matrix by varying the size of its band is entirely different from adding an extra term representing the perturbation. The difference is shown schematically in Figure 2, where Fig. 2.c corresponds to the band random matrix and Fig. 2.d represents the additive model.

The approach of band random matrices might therefore be regarded as complementary to the earlier model of additive random matrices.

In this section we discuss a generalization of the ensemble of real symmetric band random matrices investigated by Casati *et al.* [116] and complex band matrices discussed by Camarda [153]. Our model enables us to characterize all three transitions between Poisson, orthogonal, and unitary ensembles. The complex Hermitian band matrix $A_{ij} = A_{ij}^{\dagger}$ is defined by [154]:

$$A_{ij} = (\xi_{ij} + i\zeta_{ij})\,\Theta(b - |i-j|)\,, \quad i,j = 1,\ldots,N\,, \tag{23}$$

where b is the bandwidth and $\Theta(.)$ denotes the unit step function. The symbols ξ_{ij} and ζ_{ij} represent statistically independent random variables distributed according to a Gaussian distribution with zero mean and variances σ_{ij}^R and σ_{ij}^I, respectively. The parameter c measuring the effective size of the imaginary part of the off-diagonal matrix elements is determined by the condition

$$c = \frac{(\sigma_{ij}^R)^2 + (\sigma_{ij}^I)^2}{(\sigma_{ij}^R)^2}\,, \quad i \neq j\,. \tag{24}$$

All eigenvalues are kept in the constrained energy interval by imposing a normalization condition $\mathrm{Tr}\,(A^2) = N + 1$. The variances of the real and imaginary parts of the matrix elements can be thus expressed by the parameters of the model, N, b, and c:

$$(\sigma_{ij}^R)^2 = \frac{1}{c}\,\frac{(N+1)}{b(2N-b+1)}(1+\delta_{ij}) \tag{25}$$

and

$$(\sigma_{ij}^I)^2 = \frac{c-1}{c}\,\frac{(N+1)}{b(2N-b+1)}(1-\delta_{ij})\,. \tag{26}$$

For a diagonal random matrix ($b = 1$) the density of eigenvalues is Gaussian and the level spacings are distributed according to a Poisson distribution, independently of the parameter c. In the opposite limiting case of the full matrix ($b = N$), variations of the parameter c correspond to the process of time reversal symmetry breaking in a dynamical system and to the transition between orthogonal and unitary ensembles of random matrices. Several aspects of the GOE–GUE transition have already been studied [142–145]. In particular, it is known that the speed of this transition depends on the size of matrices N. However, a scaling parameter v, which determines the transitions speed independently of N, might be found. In the case discussed the theory of Pandey and Mehta [144] leads to a simple result $v = N(c-1)/(2-c)$. Our numerical data confirm existence of such scaling parameter.

For $c = 1$ the variances of the imaginary part of the matrix elements σ^I vanish and the real matrix A belongs to GOE and displays linear level repulsion. For larger values of the parameter c the matrix elements are complex but the variance of the real part is greater than the variance of the imaginary part; the probability distribution of the matrix elements on the complex plane is represented by an ellipse. An increase of the parameter c corresponds to squeezing along the larger axis of this ellipse. In the limiting case of $c = 2$ the variances of the real and imaginary parts of the off-diagonal elements are equal and the complex matrix A pertains to GUE and exhibits quadratic level repulsion. Thus in both limiting cases the value of the parameter c coincides with the degree of level repulsion.

Our preliminary results [154] show that for arbitrary values of the parameter c the level spacing distribution might be approximated by the distribution $P_t(s)$ proposed by Izrailev [124, 155]

$$P_t(s) = A\left(\frac{\pi s}{2}\right)^t \exp\left[\frac{-t\pi^2}{16}s^2 - \left(B - \frac{t\pi}{4}\right)s\right]. \tag{27}$$

The constants A and B are determined by the normalization of the distribution $\int_0^\infty P_t(s)ds = 1$ and of the mean value $\int_0^\infty sP_t(s)ds = 1$. The above formula gives the Poisson distribution for $t = 0$ and for $t = 1$ and 2 provides fair approximations to the exact GOE and GUE distributions. It is worth to note that in the limit of large values of x (full matrices) it is justified to apply the formula (18) characterizing the GOE–GUE transition. In this case this distribution provides a better approximation to the numerical data, however, the distribution (27) may be used in the entire range of the parameters b and c (or x and v) in order to characterize the nature of the level spacing distribution.

Our numerical results obtained for complex Hermitian band matrices ($c = 2$) show that the fitted value of the parameter t depends only on the scaling parameter $x = b^2/N$ as in the case of real symmetric matrices, studied in ref [118]. It is interesting to compare the results obtained for $c = 1$ (transition Poisson–GOE) and $c = 2$ (transition Poisson–GUE). We observed, for any value of the scaling parameter x, that the value of the fit parameter t_2 obtained in the latter case is approximately twice the parameter t_1 got in the former case. Both transitions are therefore correlated and the scaling parameter x controls the transitions Poisson–GOE (fitting parameter t_1 varies from 0 to 1) and Poisson–GUE (fitting parameter t_2 varies from 0 to 2) in the same manner.

The eigenvector statistics $P(y)$ may be described by the mean entropy of eigenvectors $\langle H\rangle$ given by (7) and (8). For real symmetric matrices characterized by $v = 0$ (or $c = 1$) it is convenient to compare the mean entropy with the mean entropy $\bar{H}_1$ of the matrix belonging to GOE. This

leads to the definition of averaged scaled localization length of eigenvectors [116]

$$\eta_0 = \exp(\langle H \rangle - \bar{H}_1) . \tag{28}$$

This quantity does not depend on the size of matrix N and takes values between 0 for diagonal matrix and 1 for GOE. It has been reported that the scaled localization length η_0 [116] and the eigenvector statistics [120] depend only on the scaling parameter $x = b^2/N$. A simple approximate relation, proposed in Ref. [116],

$$\eta_0 = \alpha x/(1 + \alpha x), \quad \alpha \approx 1.4 , \tag{29}$$

seems to be valid for all values of x smaller than 10.

Complex matrices with the same variances of the real and imaginary parts of elements are characterized by $c = 2$ or $v = \infty$. In order to describe the properties of the eigenvectors of matrices in this case we define the localization length η_∞ by comparing the averaged entropy of eigenvectors $\langle H \rangle$ with the entropy $\bar{H}_2$ of GUE,

$$\eta_\infty = \exp(\langle H \rangle - \bar{H}_2) . \tag{30}$$

Throughout the transition Poisson–GUE the localization length $\eta_\infty = \eta_\infty(N, b)$ varies form zero to unity. Our numerical experiments show that η_∞ depends on the same scaling variable $x = b^2/N$.

The localization length might be generalized for the interpolating case determined by $0 < v < \infty$:

$$\eta_v = \exp\left[\langle H(N, b, v) \rangle - \bar{H}(N, b = N, v)\right] . \tag{31}$$

Note that in the particular cases of $v = 0$ and $v = \infty$ the generalized localization length η_v reduces to the previous definitions (28) and (30), applicable to the cases of orthogonal and unitary ensembles respectively.

We performed a detailed investigation of the model described above by analyzing complex band random matrices of size varying from 100 to 1000. The number of constructed matrices was determined by the requirement of accumulating at least 25,000 eigenvalues or $3*10^6$ eigenvector components in each sample. We found the existence of the same scaling parameter $x = b^2/N$ for arbitrary values of the parameter v, which controls the effects of time reversal symmetry breaking. Moreover, the functional dependence of the generalized localization length η_v on the scaling parameter x might be approximated by the relation (29) with parameter α depending on v. Figure 5 presents this dependence for real symmetric matrices and complex Hermitian matrices for several sizes of matrices N. The entropy $\langle H \rangle$ was averaged over the half of eigenvectors corresponding to eigenvalues from the center of the spectrum.

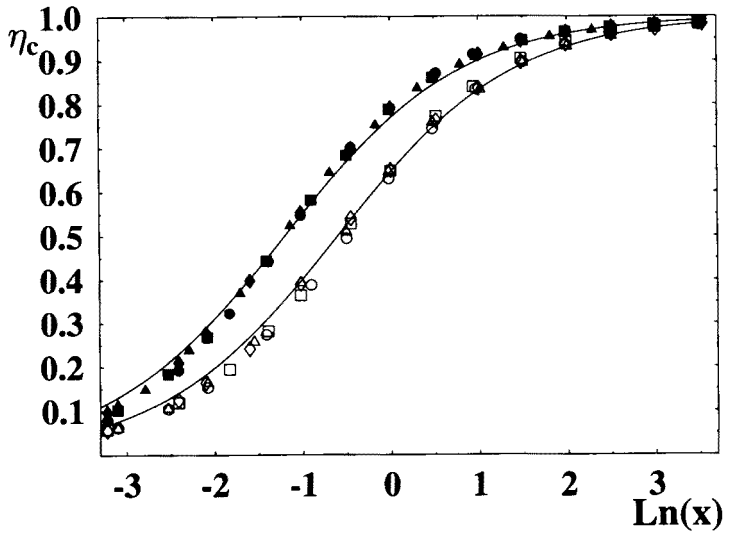

Fig. 5. Mean entropy of central eigenvectors for the complex Hermitian band matrices plotted against the scaling variable $x = b^2/N$ for $c = 1.0$ (transition Poisson–GOE — lower curve) and $c = 2.0$ (transition Poisson–GUE — upper curve). Solid lines represent formula (29) with α fitted. Matrix size N equals to 100 (○), 200 (□), 400 (◇), and 800 (△).

Scaling laws found in complex band random matrices enable us to treat this model as a possible candidate for an ensemble of random matrices describing changes of the properties of quantum dynamical systems during the processes of time reversal symmetry breaking or transitions between regular and chaotic dynamics. Note that the same scaling parameter x describes, for arbitrary value of the parameter v, statistical properties of the eigenvalues of Hermitian band random matrices (level spacing distribution), as well as the properties of eigenvectors (localization length).

3. Statistical properties of quantum dynamical systems

3.1. Eigenvalues

The correspondence between the character of the dynamics of classical systems and the statistical properties of the spectrum of their quantum analogues is well established [11, 12, 20]. The level statistics of the spectrum of a generic classically regular system is given by the Poisson distribution [74, 156, 157], while classically chaotic systems display level repulsion and the level distribution well approximated by one of the Wigner surmises (2)–(4), depending on the symmetry of the system. However, there are exceptions from this rule.

The spectrum of the quantum one dimensional harmonic oscillator is equidistant, so the level distribution is singular: $P(s) = \delta(1)$. Furthermore, the spectrum of the two-dimensional harmonic oscillator with incommensurate frequencies is closer to a Poisson distribution, and this distribution is approached for the large number of degrees of freedom of the oscillator [158]. Likewise one of the simplest integrable systems — the square billiard — does not possess a Poisson spectrum. For a rectangular billiard the degeneracy is shifted, and in the generic case of incommensurate sides of the billiard the level statistics might be approximated by the Poisson distribution [159–161].

There exist also integrable systems which display a spectrum characteristic of canonical ensembles of random matrices. A specific example of a regular system with a GOE-like spectrum was proposed in [162]. This model consists of a particle moving in a one-dimensional potential well, which might be considered as a distorted quadratic well of the harmonic oscillator. It seems even possible to construct in a similar manner a regular, integrable system displaying any given statistical properties of the spectrum. It has been also pointed out [163], that due to finite numerical accuracy one may find a Wigner-like level distribution in the spectrum of quantized integrable systems.

We have mentioned some examples of regular systems which *do not* display Poisson statistics in their spectrum. On the other hand there exist classically chaotic systems which *do* possess a Poisson-like spectrum. This feature is associated with the effect of *dynamical localization* [65, 164], and was found in the model of the quantum kicked rotator [121, 165–167]. It is also known [168] that the elongated, composed billiard build of several parts of arbitrary shapes joined together by narrow channels, displays a Poisson level distribution. This fact may be easily understood, when considering the limiting case of infinitesimally narrow channels. The original composed billiard can be than considered as a set of decoupled chaotic billiards. The spectrum of this system is thus equivalent to the superposition of several GOE spectra and has therefore the Poisson-like properties.

The above list of some exceptional cases does not mean that there is no link at all between the dynamics of classical systems and the spectral properties of their quantum analogues. The level spacing distribution of typical quantized chaotic systems conforms with such a high accuracy to the exact distribution resulting from appropriate ensembles of random matrices that even small discrepancy between the numerical data obtained for a dynamical system and the approximate Wigner surmise was reported [169]. In addition, quantities measuring long range correlations of the spectra of quantum dynamical systems, such as the spectral rigidity $\Delta_3(L)$ or the number variance $\Sigma^2(L)$, were found to be faithful to the predictions of

ensembles of random matrices, at least for small values of the range L [20, 23].

3.2. Eigenvectors

The statistical properties of the eigenvectors $|\psi_i\rangle$ of a Hamilton operator $\widehat{A}$ representing a quantum dynamical system can be described by the distribution $P(y)$ of the squared components $y = |\langle\psi_i|l\rangle|^2$, where $|l\rangle, l = 1, \ldots, N$ is an arbitrary orthonormal basis in N dimensional Hilbert space. The eigenvector statistics $P(y)$ has an obvious advantage compared to the level spacing distribution $P(s)$ measuring the properties of the spectrum: the former statistics contains an N times larger sample of numerical data than the latter. This superiority is, however, balanced by an important deficiency: the eigenvector statistics is basis dependent. For example, if the basis $\{|l\rangle\}$ is taken as the eigenbasis of the Hamiltonian $\widehat{A}$, the eigenvector statistics is singular and carries no information at all. Moreover, there exists no one-to-one correspondence between the statistical properties of eigenvalues of a Hamiltonian matrix and the properties of its eigenvectors. It is possible, in fact, to construct a matrix A_r representing some Hamiltonian with any wished eigenvector statistics, independently of level spacing distribution. Let A_d denotes a diagonal matrix, described by a level spacing distribution $P_d(s)$ and U stands for an unitary matrix with elements characterized by a distribution $P_m(|U_{ij}|^2)$. The rotated matrix $A_r = U^\dagger A_d U$ possesses thus the eigenvector statistics $P_m(y)$ independently of the level spacing distribution $P_d(s)$. This simple example shows that one has to be cautious analyzing and interpreting the distribution of eigenvectors of a dynamical system. It is not at all clear, how to select, for a given quantum system, an "appropriate basis", which allows us to extract form the statistics of eigenvectors a relevant information concerning the dynamical properties of the system.

The eigenvector statistics has often been calculated in the eigenbasis of the unperturbed Hamiltonian [170, 171]. It has been observed [4, 171] that in an appropriate basis, the eigenvector statistics for a quantum chaotic system (for a large dimension N of Hilbert space) can be described with great accuracy by a Porter–Thomas distribution (6), or, depending on the symmetry of the system, by a χ^2 distribution, typical of canonical ensembles of random matrices [16, 18, 172]. We shall call such a basis *random* with respect to the system. In order to describe the eigenvector statistics for the transition from chaotic to regular dynamics it has been proposed to use the same χ^2_β distribution and allow the number of degrees of freedom β to take any rational value between zero and unity [173, 136]. There are no strict physical arguments supporting this conjecture. However, this distribution

seems to reproduce in a qualitative manner the behaviour of the eigenvector statistics with values of the parameter β decreasing parallel to the corresponding classical transition from chaotic to regular motion. In a descriptive language, a matrix of eigenvectors, "dense" it the case of classically chaotic motion, becomes "sparse" for dynamical systems corresponding to regular motion.

The most natural application of the Porter Thomas distribution (6) refers to the eigenvectors of a Hamiltonian $\widehat{A}$, describing an autonomous dynamical system, or a Floquet operator $\widehat{F}$, representing a time-dependent periodical system, in some fixed basis. In a similar manner, this distribution describes the statistical properties of an expansion of some arbitrarily chosen state $|\phi\rangle$ in the eigenbasis of the operators $\widehat{A}$ or $\widehat{F}$. Let us consider an observable $\widehat{B}$. The arbitrary state $|\phi\rangle$ may be generated from an eigenvector $|\psi_i\rangle$ of $\widehat{A}$ by

$$|\phi\rangle = \frac{\widehat{B}|\psi_i\rangle}{\sqrt{|\langle\psi_i|\widehat{B}\widehat{B}^\dagger|\psi_i\rangle}}. \tag{32}$$

This choice of the state $|\phi\rangle$ is made because its components $\langle\psi_k|\phi\rangle \sim \langle\psi_k|\widehat{B}|\psi_i\rangle$ define transition strengths by $y = |\langle\psi_k|\phi\rangle|^2$. The strengths of transitions between the eigenstates of a quantum system might be measured experimentally in some cases. Results obtained in the absorption experiments in nuclei [17] and atoms [55] show that the measured probability distribution of transition strengths agrees with predictions from ensembles of random matrices. Similar results were also obtained by numerical analysis of model quantum systems such as coupled spins [173, 174], coupled Morse oscillators [175] and the kicked top [136]. Several features of the matrix element distribution are universal for all quantum chaotic systems and may be explained by means of ensembles of random matrices. In addition there exist system-specific properties of matrix element distribution. A semiclassical theory [176, 177], linking them to the classical periodic orbits, has recently been developed [178].

The problem of selecting an "appropriate" basis for the eigenvector statistics of the given Hamiltonian $\widehat{A}$ is closely related to the question, of which operators $\widehat{B}$ can have their matrix element distribution described by the predictions of random matrices. None of the operators commuting with the Hamiltonian belong to this group, since their matrix representation in the eigenbasis of $\widehat{A}$ might be diagonal. This observation suggests that a partial answer to this question may be obtained by measuring the degree of noncommutativity between the Hamiltonian $\widehat{A}$ and the observable $\widehat{B}$. Such a method has recently been applied [179] for the case of periodic systems described by a unitary Floquet operator $\widehat{F}$.

Let $\widehat{B}^{(l)}$ denote the image of $\widehat{B}$ after l periods of a system $\widehat{F}$

$$\widehat{B}^{(l)} = \widehat{F}^{\dagger l}\widehat{B}\widehat{F}^{l}. \tag{33}$$

We apply the standard definition of the scalar products in operator space $\langle\widehat{A}|\widehat{B}\rangle = \mathrm{Tr}(\widehat{A}^{\dagger}\widehat{B})$, and define a *random operator*. An operator $\widehat{B}$ is random with respect to the system described by the unitary evolution operator $\widehat{F}$, if it is orthogonal to its images for any time l, *i.e.*

$$\langle\widehat{B}^{(l)}|\widehat{F}^{\dagger}\widehat{B}^{(l)}\widehat{F}\rangle = 0. \tag{34}$$

It has been conjectured, and by a numerical simulation verified [178], that the distribution of matrix elements of an operator $\widehat{B}$ random with respect to a system $\widehat{F}$ is given by the χ^2_β distribution which is characteristic of random matrices.

Note that the above reasoning might also be generalized to autonomous systems described by a Hermitian operator $\widehat{A}$. In a similar manner we may treat the problem of describing the distribution of the eigenvectors of a Hamiltonian system $\widehat{A}_1$ represented in the eigenbasis of an operator $\widehat{A}_2$.

Eigenvector statistics may also be used to study local properties of the quantum system. To that end it is convenient to take coherent state $|\alpha_{\bar{x}}\rangle$, localized at a point $\bar{x}$ of classical phase space, and to examine its expansion in the eigenbasis of the system. It has been observed [132] that there exists a correlation between the number of relevant components of the coherent state in this expansion and the character of the dynamics of the corresponding classical system in vicinity of the point $\bar{x}$. Moreover, the circumstances under which the distribution of the components of a coherent state might be described by the χ^2_β distribution has been analysed [180, 181]. Note that in contrast to the eigenvector statistics, the distribution of components of coherent states in the eigenbasis of the system is defined without any arbitrariness (except for the definition of coherent states).

The distribution of the components of a coherent state in the eigenbasis of a system carries information concerning the structure of the eigenfunctions. Typical eigenfunctions of a quantum chaotic system are irregular and do not display any spatial structure [182–184]. However, it has been discovered by Heller [185] that some eigenfunctions exhibit structures correlated with periodic orbits in the corresponding classical system. These objects, called *quantum scars*, have been investigated in numerous recent papers [22, 186–193]. It has been proposed that the distribution of the components of coherent states be analysed in order to detect quantum scars [194]. Discrepancies between the observed statistics of the components of a coherent state $|\alpha_{\bar{x}}\rangle$ and the Porter–Thomas distribution tell us about a localization

of eigenstates in the vicinity of the point $\bar{x}$, and thus allows us to assert that *some* eigenstates of the Hamiltonian are scarred by a classical periodic orbit passing close to the point $\bar{x}$. It has been conjectured that the presence of quantum scars may influence not only the eigenvector statistics but also the statistical properties of the spectrum and the curvature distribution [102].

3.3. Parametric dynamics

Let us discuss the motion of the eigenvalues of the Hamiltonian (1), considering the parameter λ as a fictitious time [88, 89]. The eigenvalues $\{x_k\}$ of the Schrödinger equation,

$$\widehat{A}(\lambda)|\psi_k(\lambda)\rangle = x_k(\lambda)|\psi_k(\lambda)\rangle; \quad k = 1, \ldots, N, \tag{35}$$

might be interpreted as positions of the particles moving in a one dimensional space, while the derivatives $dx_k/d\lambda$ play the role of the momenta of the particles. We denote the diagonal elements p_k the matrix V by

$$p_k(\lambda) = \langle\psi_k(\lambda)|\widehat{V}|\psi_k(\lambda)\rangle \tag{36}$$

and the scaled off-diagonal elements L_{kl} by

$$L_{kl}(\lambda) = [x_k(\lambda) - x_l(\lambda)]\langle\psi_k(\lambda)|\widehat{V}|\psi_l(\lambda)\rangle\,. \tag{37}$$

If V pertains to the orthogonal ensemble, one may find a representation in which the coupling strengths L_{kl} are real. For V belonging to the unitary ensemble the coupling strengths are complex, and in the case of the symplectic ensemble, L_{kl} have a quaternion structure. Introducing a unified notation, we write $L_{kl} = \sum_{i=1}^{\beta} L_{kl}^{(i)}$ with $\beta = 1, 2$, and 4 for the orthogonal, unitary and symplectic cases, respectively.

Assuming that for $\lambda = 0$ no degeneracy in the system $\widehat{A}$ occurs and that for arbitrary values of the parameter λ the eigenvectors are orthonormal, $\langle\psi_k(\lambda)|\psi_l(\lambda)\rangle = \delta_{kl}$, it is possible [88–91] to derive a set of equations governing the motion of the eigenlevels $\{x_k, k = 1, \ldots, N\}$:

$$\frac{dx_k}{d\lambda} = p_k\,, \tag{38}$$

$$\frac{dp_k}{d\lambda} = 2\sum_{l\neq k}\frac{L_{kl}L_{lk}}{(x_k - x_l)^3}\,, \tag{39}$$

$$\frac{dL_{kl}}{d\lambda} = \sum_{n\neq k,l} L_{kn}L_{nl}\left(\frac{1}{(x_k - x_n)^2} - \frac{1}{(x_l - x_n)^2}\right). \tag{40}$$

The above equations of motion might be generated from the following Hamiltonian

$$\mathcal{H}_{\mathrm{CM}} = \tfrac{1}{2}\sum_{k=1}^{N} p_k^2 + \tfrac{1}{2}\sum_{k\neq l}^{N}\sum_{i=1}^{\beta}\frac{(L_{kl}^{(i)})^2}{(x_k - x_l)^2}\,, \tag{41}$$

which describes the dynamics of a set of N classical interacting particles. This is known in the literature [94, 195] as the generalized Calogero–Moser system (CM). The motion takes place in $\beta(N-1)N/2 + 2N$ dimensional phase space and the system has been shown to be integrable [94]. Note that the motion is unbounded in space and, in the limit $\lambda \to \infty$, particles may escape to infinity. On the other hand, quantum systems of the form of equation (11) or (20) lead to level dynamics equivalent [11, 197] to the classical Hamiltonian

$$\mathcal{H}_{mCM} = \tfrac{1}{2}\sum_{k=1}^{N}(p_k^2 + x_k^2) + \tfrac{1}{2}\sum_{k\neq l}^{N}\sum_{i=1}^{\beta}\frac{(L_{kl}^{(i)})^2}{(x_k - x_l)^2}\,. \tag{42}$$

This modified Calogero–Moser Hamiltonian differs from (41) by an harmonic oscillator potential $\sum_k x_k^2/2$, which is responsible for binding the gas of particles together.

The level dynamics approach might also be used for periodically kicked systems represented by an unitary Floquet operator $\widehat{F}_0$ and a Hermitian perturbation operator $\widehat{V}$,

$$\widehat{F}(\lambda) = \widehat{F}_0 \exp(i\lambda\widehat{V})\,. \tag{43}$$

The role of the particles is played in this case by quasi-energy eigenphases φ_k defined in the interval $(0, 2\pi\rangle$ by

$$\widehat{F}(\lambda)|\psi_k(\lambda)\rangle = \exp[i\varphi_k(\lambda)]|\psi_k(\lambda)\rangle;\quad k = 1,\ldots,N\,. \tag{44}$$

It is necessary to modify equation (37) for this case and to define the coupling strengths L_{kl} as [11]

$$L_{kl}(\lambda) = \sin\left(\frac{\varphi_k - \varphi_l}{2}\right)\langle\psi_k(\lambda)|\widehat{V}|\psi_l(\lambda)\rangle\,. \tag{45}$$

The level dynamics is described by a set of differential equations analogous to (38)–(40),

$$\frac{d\varphi_k}{d\lambda} = p_k\,, \tag{46}$$

$$\frac{dp_k}{d\lambda} = \sum_{l\neq k} L_{kl}L_{lk}\frac{\cos\left(\frac{\varphi_k-\varphi_l}{2}\right)}{\sin^3\left(\frac{\varphi_k-\varphi_l}{2}\right)}\,, \tag{47}$$

$$\frac{dL_{kl}}{d\lambda} = \tfrac{1}{2}\sum_{n\neq k,l} L_{kn}L_{nl}\left(\frac{1}{\sin^2\left(\frac{\varphi_k-\varphi_n}{2}\right)} - \frac{1}{\sin^2\left(\frac{\varphi_n-\varphi_l}{2}\right)}\right). \tag{48}$$

The above system of equations of motion might be generated [11] from the classical Hamiltonian

$$\mathcal{H}_S = \tfrac{1}{2}\sum_{k=1}^{N} p_k^2 + \tfrac{1}{2}\sum_{k\neq l}^{N}\sum_{i=1}^{\beta} \frac{(L_{kl}^{(i)})^2}{\sin^2(\varphi_k - \varphi_l)}. \tag{49}$$

This Hamiltonian is strictly integrable and is known as the generalized Sutherland system [94, 95]. Its generalization has been proposed [198], which would correspond to quantum periodically driven systems.

Since the classical Hamiltonians $\mathcal{H}$ representing the level dynamics are integrable, it is possible to get the equations of motion for each eigenvalue $x_i(\lambda)$ (or eigenphase $\varphi_i(\lambda)$) of the quantum system under investigation. However, it has been shown [199] that it is usually easier and more efficient to diagonalize a $N \times N$ matrix numerically than to solve a set of $\beta(N-1)N/2+2N$ coupled ordinary differential equations. The standard technique of obtaining the levels of a quantum system by diagonalizing the matrix representation of its Hamiltonian, seems, for practical reasons, to be more useful than the level dynamics. On the other hand, it is worth noting that the eigenvalues of a *non-integrable* quantum system, can, in principle, be obtained by analysis of an appropriate *integrable* classical Hamiltonian describing the motion of the energy levels.

The systems of differential equations (38)–(40) and (46)–(48) are called *level dynamics*. In addition to the parametric motion of the eigenvalues, they describe the rotation of eigenvectors in orthogonal (unitary or symplectic) space. Differentiating equation (44) with respect to the parameter λ and multiplying it by an eigenvector $\langle\psi_n|$ we get

$$\langle\psi_n|\frac{d|\psi_k\rangle}{d\lambda} = \frac{-iV_{nk}}{1-\exp[-i(\varphi_k-\varphi_n)]}. \tag{50}$$

This relation enables us to obtain an estimate of the magnitude of components of the eigenvector $|\psi_k(\lambda_1)\rangle$, in the eigenbasis representation of $\widehat{F}(\lambda+\Delta\lambda)$. For small values of the rotation parameter $\Delta\lambda$ the squared off-diagonal component $y = |\langle\psi_k(\lambda)|\psi_n(\lambda+\Delta\lambda)\rangle|^2$ reads

$$y = (\Delta\lambda)^2 \frac{|V_{kn}|^2}{2(1-\cos[\varphi_k-\varphi_n])} + o((\Delta\lambda)^3). \tag{51}$$

This equation shows that the eigenvector statistics in the rotated basis $P_\Delta(y)$ is correlated with the level spacing distribution, which determines the cosine term, and the distribution of the elements of the perturbation matrix $|V_{kn}|^2$. Moreover, it explains why the Shannon entropy H_Δ of a

rotated eigenvector is proportional, for small values of $\Delta\lambda$, to square of the rotation parameter.

4. A representative dynamical system — the periodically kicked top

4.1. Definition and properties of the model

The time evolution of a periodically driven system is described by a unitary Floquet operator $\widehat{F}$. In the case of a periodically kicked system, described by a Hamiltonian

$$\widehat{A} = \widehat{A}_0 + k\widehat{V} \sum_{n=-\infty}^{n=+\infty} \delta(t/t_0 - n), \tag{52}$$

the form of the operator $\widehat{F}$ is particularly simple:

$$\widehat{F} = \exp(-ik\widehat{V}) \exp(-it_0 \widehat{A}_0). \tag{53}$$

The perturbation operator $\widehat{V}$ is assumed to be Hermitian, t_0 is the perturbation period, and the kicking strength k plays the role of the fictitious time λ in the level dynamics (43)–(49). Studies of the quantum signatures of chaos were initiated with an analysis of the quantum kicked rotator [1]; after a decade it is one of the best known quantum models [2, 3, 12, 50, 65, 121, 149, 164–167]. Apart of a peculiar case of *quantum resonance* [200–202], the quantum dynamics of the kicked rotator is described in an infinite-dimensional Hilbert space. In order to perform a numerical investigation of the system a technique for producing a finite sized unitary matrix of a finite size is required. This problem does not occur for those quantum models for which the Hilbert space might be decomposed into independent subspaces of finite size. The model of the periodically kicked top [15, 128, 129] belongs to this class and is extensively used to study various aspects of quantum chaos [1, 9, 100, 102, 108, 130–134, 179, 203–207]. Since several versions of the model, pertaining to all three different universality classes, are known [15, 21, 132], we have chosen this system for numerical investigation.

The three components $\widehat{J}_i$, $i = 1, \ldots, 3$ of the angular momentum operator $\widehat{J}$ are the dynamical variables of periodically kicked top models. They obey the commutation relation $[\widehat{J}_i, \widehat{J}_j] = i\epsilon_{ijk}\widehat{J}_k$. The operators $\widehat{A}_0$ and $\widehat{V}$, defining the Floquet operator (53), are arbitrary functions of $\widehat{J}_i$, $i = 1, 2, 3$. If both operators are linear functions of one component, the resulting dynamics is integrable [11]. On the other hand, if at least one of the operators

$\hat{A}_0$ and $\hat{V}$ is quadratic in $\hat{J}_i$, for sufficiently large values of the kicking strength k the corresponding classical system is chaotic [15].

We shall thus be concerned with the simplest version of the model defined by

$$\hat{A}_0 = p\hat{J}_z\,; \qquad \hat{V} = \frac{\hat{J}_x^2}{2j}\,, \tag{54}$$

which can be represented by the Floquet operator

$$\hat{F}_o = \exp\left(\frac{-ik\hat{J}_x^2}{2j}\right)\exp(-ip\hat{J}_z)\,, \tag{55}$$

where p and k are the parameters of the model. The eigenvalue $j(j+1)$ of the operator $\hat{J}^2$ fixes the dimension of the Hilbert space N as $N = 2j+1$. It is convenient to analyse the system in the eigenbasis of the operator $\hat{J}_z$, $|j,m\rangle$, $m = -j,\ldots,j$.

The perturbation operator $\hat{V}$, quadratic in $\hat{J}_x$, does not couple states $|j,m\rangle$ of different parity and the operator F_o breaks down into a block diagonal form of size j and $j+1$. Both subspaces are dynamically independent and numerical calculations can be performed separately for each parity. For even integer j an additional symmetry appears for $p = \pi/2$ and the $j+1$ parity is decoupled into blocks of sizes $j/2$ and $j/2+1$.

The semiclassical regime of the model is achieved for $j \gg 1$. It is difficult to handle matrices of size greater than, say, 2000 and to perform an exact numerical analysis of this regime of the model. On the other hand, it is easy to find [15], in the limit $j \to \infty$, a classical system corresponding to the model (54). The normalised vector $\bar{X} = \bar{J}/j$ lies, in the limit, on the unit sphere and the time evolution can be given by a map for the three components (X,Y,Z) of the angular momentum vector. The classical map $\bar{X}' = M(\bar{X})$ reads [15]

$$\begin{aligned} X' &= X\cos p - Y\sin p\,,\\ Y' &= (Y\cos p + X\sin p)\cos(kX') - Z\sin(kX')\,,\\ Z' &= (Y\cos p + X\sin p)\sin(kX') + Z\cos(kX')\,. \end{aligned} \tag{56}$$

The above transformation maps the position of the top between successive kicks. Since the norm of vector $\bar{X}$ is conserved the dynamics of the system can be represented by a two dimensional phase space, equivalent to a sphere. In the case of zero perturbation parameter k the system is integrable and the classical map (56) represents a rotation along the z axis.

For non-zero values of k, a chaotic layer appears in the vicinity of the unstable fixed points in the phase space. Sufficiently large kicking strength

breaks down the last KAM lines and the domains of chaotic motion are connected. The critical value of the perturbation strength k_c increases with the parameter p in the interval $p \in (0, \pi/2)$. For $p \sim \pi/2$ chaotic dynamics dominates for $k \sim 3.0$, while for $k = 6.0$ the entire phase space is covered with chaotic motion ($r = 1.0$).

Classical chaotic dynamics might be characterized by the Lapunov exponent Λ, measuring the exponential divergence $d(t)$ of neighbouring trajectories in phase space. We iterated the map (56) for several initial values. In order to estimate the value of Λ we used the standard definition [5, 6, 12, 208]

$$\Lambda = \lim_{T \to \infty} \lim_{d(0) \to 0} \frac{1}{T} \ln \frac{d(T)}{d(0)} . \tag{57}$$

Numerical efficiency was improved by an application of Bennetin's "sawtooth" technique [209]. A fair approximation to Λ is provided by taking 10^3 iterations of the map; the results obtained become stable for 10^5 iterations. To characterize the entire dynamical system we averaged values of Λ over the phase space, excluding the islands of stability. The average was calculated for all values of Λ greater than a threshold, (settled arbitrarily to 0.01), which initial points localized into regular islands. Since the number of chaotic trajectories increases with the kicking strength, the accuracy of the estimation of Λ is worst for small values of k.

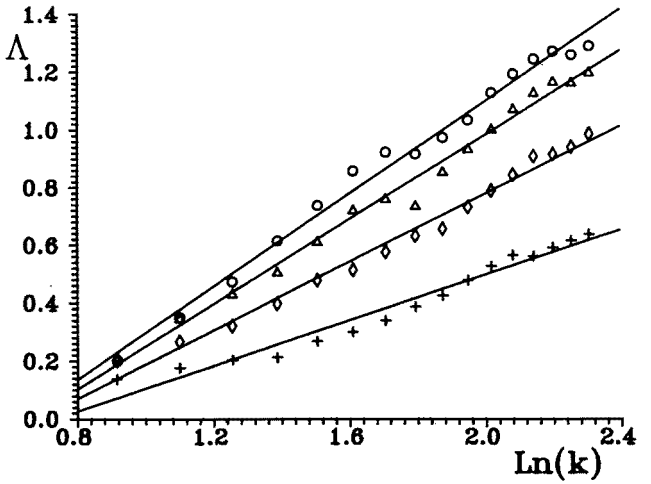

Fig. 6. Classical kicked top. Average value of Lapunov exponent Λ, plotted against the kicking strength for $p = 0.4(+)$, $p = 0.7(\diamond)$, $p = 1.0(\triangle)$, $p = 1.3(\bigcirc)$.

Figure 6 presents the dependence of the Lapunov exponent on the kicking strength k for four values of the parameter $p = 0.4, 0.7, 1.0, 1.3$. The

kicking strength is represented on a logarithmic scale. As shown in the picture, a straight line gives a reasonable approximation in each case. A linear best fit gives the following values of the slope: $0.39, 0.59, 0.73, 0.80$, in the order of increasing p.

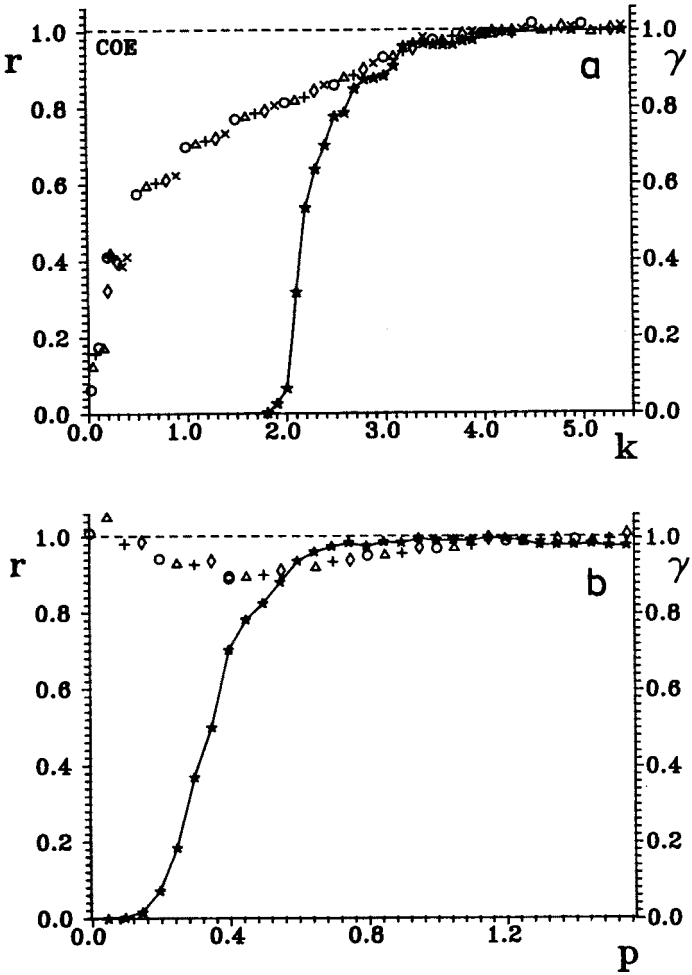

Fig. 7. Fraction of the classical phase space covered by chaotic dynamics ((⋆) joined by solid line) plotted a) against kicking strength k for fixed $p = 1.3$; b) against parameter p for fixed $k = 4.0$. Entropy of eigenvectors γ of the corresponding quantum model obtained in (a) for $j = 200(\bigcirc)$, $j = 160(\triangle)$, $j = 100(+)$, $j = 70(\diamond)$, $j = 40(\times)$ and in (b) for $j = 200(\bigcirc)$, $j = 150(\triangle)$, $j = 100(+)$, $j = 50(\diamond)$.

The classical map is periodic with respect to the parameter p, since $M(p, k) = M(p + 2\pi, k)$. The quantum dynamics described by the operator (55) is also periodic with respect to the parameter k and the period is equal

to $4\pi j$. In the limit $j \to \infty$ this quantity tends to infinity, so the classical map M is not periodic in k. In spite of this difference in the role played by both parameters, one may fix the value of k and treat p as a perturbation parameter. Analyzing the dependence of the Lapunov exponent on p we found a similar logarithmic relation $\Lambda \sim \log(p)$ (for $p < 1$ with large enough values of k). This observation is consistent with the well-known properties of the standard map [6]. It has been shown that in the limiting case of $p \to 0$, $k \to \infty$ the quantum kicked top tends to the quantum kicked rotator, provided that the product pk is kept constant [204]. A similar relationship exists between the corresponding classical models. In this limit the classical kicked top becomes equivalent to the classical kicked rotator with the kicking strength K equal to pk. For the standard map, which governs the dynamics of the kicked rotator, the Lapunov exponent Λ grows logarithmically with the kicking strength K [208].

For a fixed value of p the fraction of the phase space r covered by layers of chaotic motion increases monotonously with the perturbation parameter k. Such dependence is presented in Fig. 7.a for $p = 1.3$. Numerical data, marked by stars, are joined by a solid line. The area of chaotic motion grows rapidly at $k = 2.0$ and accomplishes the half of the phase space at $k_{0.5} \sim 2.2$. For $k = 3.0$ only some minor islands of stability exists, while the transition from to chaotic motion is practically completed at $k \sim 4.0$. For $p < 1$ the characteristic value $k_{0.5}$ is approximately equal to $1.4/p$, while for $1.2 < p < 1.8$ the dependence $k_{0.5}$ on p is weak.

Figure 7.b shows complementary results obtained for a fixed value of $k = 4.0$ with changing values of the parameter p. The percentage of chaotic trajectories r starts to grow at $p \sim 0.2$ and achieves 50% for $p_{0.5} \sim 0.35$. Thus the qualitative nature of the dependencies of r on each of the two parameters k and p is similar.

4.2. Transition Poisson–orthogonal

For the model of orthogonal kicked top, defined by the Floquet operator (55), there exists a generalized time-reversal symmetry $\widehat{T}$, such that $\widehat{T}\widehat{F}_o = \widehat{F}_o^{-1}\widehat{T}$. The symmetry operator $\widehat{T}$, expressed by the conjunction operator $\widehat{K}c|\psi\rangle = c^*|\psi\rangle^*$, reads [15]

$$\widehat{T} = \mathrm{e}^{ip\widehat{J}_z}\mathrm{e}^{i\pi\widehat{J}_x}\widehat{K}\,. \tag{58}$$

Due to the existence of the antiunitary symmetry $\widehat{T}^2 = -1$, the Floquet operator F_o pertains to the circular orthogonal ensemble [15, 132] under the conditions of classical chaos. It has been verified [15, 169] that for large enough values of the parameters p and k the level spacing distribution

$P(s)$ complies with the distribution typical of the orthogonal ensemble. It has also been shown [171] that the eigenvector statistics of F_o, (calculated in the eigenbasis of the unperturbed system), is given by the distribution characteristic of the orthogonal ensemble, which in the limit $j \to \infty$ tends to the Porter–Thomas distribution [136]. The mean Shannon entropy $\langle H \rangle$ of the eigenvectors of F_o, characterizing the distribution of eigenvectors, accurately agrees with the value $\bar{H}_1$, calculated according to expression (9) for the orthogonal ensemble.

For zero kicking strength k, the matrix F_o is diagonal and belongs to the Poisson ensemble. Thus the variation of the parameter k in the definition (55) allows us to study the transition between Poisson and orthogonal ensembles based on the parametric dynamics of a quantum system. The computed value of the mean entropy might be used to characterize the properties of a quantum system during the transition. In addition to the classical quantity r, Figure 7 presents the scaled entropy $\gamma = \langle H \rangle / \bar{H}_1$, obtained from quantum calculations. The scaled entropy increases with the size of matrix, which is governed by the quantum number j. This dependence is, however, rather weak. The numerical results, obtained for $p = 1.3$ and $j = 40, 70, 100, 160$, and 200 and displayed in Figure 7.a, are situated close to a single line. Observe that an increase of the mean entropy occurs for values of the kicking strength k which are smaller than the jump in the fraction of the phase space covered by classically chaotic dynamics.

The data for the scaled mean entropy γ, shown in Fig. 7.b, are obtained for $k = 4.0$ and $j = 50, 100, 150, 200$. All the points are also located along a line, but the character of the two pictures is different. Only for $p > 0.5$ does an increase of γ correspond to growth of r and might be interpreted as a signature of chaos. Moreover, for small values of the perturbation parameter p, the entropy does not tend to zero, as in Fig. 7.a. This fact might be explained by considering the choice of basis used to compute the entropy of the eigenvectors of $\widehat{F}_o$. The eigenbasis of the operator $\widehat{J}_z$, (the eigenbasis of the system with $k = 0$), which is appropriate for analysing the influence of growth of the kicking strength k, is not suitable for description of the properties of the quantum system for small values of p. In this case one could use instead the eigenbasis of $\widehat{J}_x$ (the eigenbasis of $\widehat{F}_o$ with $p = 0$). In other words, the values of γ close to unity at the upper left corner of Fig. 7.b, are not correlated with the dynamical properties of the classical system, but rather, with the choice of the basis used for computation of the eigenvectors.

Let us discuss the properties of the spectrum of $\widehat{F}_o$ during an increase of the kicking strength. A preliminary investigation of the spectrum requires about 10^3 levels. For a more precise analysis a sample consisting of circa 10^4 eigenvalues is needed, while a sample of order 10^5 levels allows us to

distinguish the fine difference between the Wigner surmise and the exact COE formula for the level spacing distribution [169]. Being unable to obtain so many levels in a single quantum system, we decided to collect data for several systems having similar properties. Doing this one has to compromise between two contradictory factors: on one hand the difference in one system parameter has to be large enough to assure the statistical independence of both spectra. On the other hand, a large difference in a system parameter between two systems makes the assumption of similar spectral properties questionable. Moreover, it is not easy to verify the latter assumption by analyzing the sets of levels of the two systems, each of which contains 100 levels.

In order to analyze the transition between the Poisson-like and Wigner-like level spacing distributions we fixed the value of the parameter $p_a = 1.3$, and varied the kicking strength k. In the vicinity of p_a the fraction of the chaotic phase space r and the entropy γ depend only weakly on p. For fixed classical parameters of the system p and k, the spectra obtained for j and $j+1$ are not correlated. In addition, the mean entropy of eigenvectors γ does not change dramatically with the quantum number j: the relative difference of the entropy between $j = 119$ and $j = 100$ is of the order of $3 * 10^{-3}$. Based on these observations, we took the risk of putting the data from 300 matrices together (obtained for $j = 100, 101, \ldots, 119$ and $p = 1.23, 1.24, \ldots, 1.36, 1.37$) in order to analyse the level spacing distribution for samples containing about 32 000 spacings each.

Figure 8 presents histograms $P(s)$ obtained for three different values of k. Classically chaotic dynamics ($r = 1$) for the system $\widehat{F}_o$ with $k = 5.0$ manifests itself in the Wigner-like level spacing distribution. For smaller values of k the fraction r of the phase space covered by chaotic dynamics decreases. Therefore it is natural to use the Berry–Robnik distribution [125]

$$P_b(s) = (1-b)^2 \exp(-s(1-r))\operatorname{erfc}\Big(\frac{\sqrt{(\pi)}bs}{2}\Big) + 2\Big[b(1-b) + \frac{\pi b^3 s}{2}\Big] \exp\Big(-s(1-b) - \frac{\pi b^2 s^2}{4}\Big), \quad (59)$$

where $\operatorname{erfc}(x)$ is the error function [139] and the parameter b, varying from zero to unity, can be interpreted as the fraction r describing the dynamics of the corresponding classical system. A best fit of the distribution (59) to the numerical data, represented by dashed lines in the figure, is far from satisfactory. Likewise, the distribution (14), originating from the additive model of random matrices, is not adequate in this case. On the other hand the Brody distribution [16]

$$P_q(s) = (1+q)B(q)s^q \exp\big(-B(q)s^{1+q}\big), \quad (60)$$

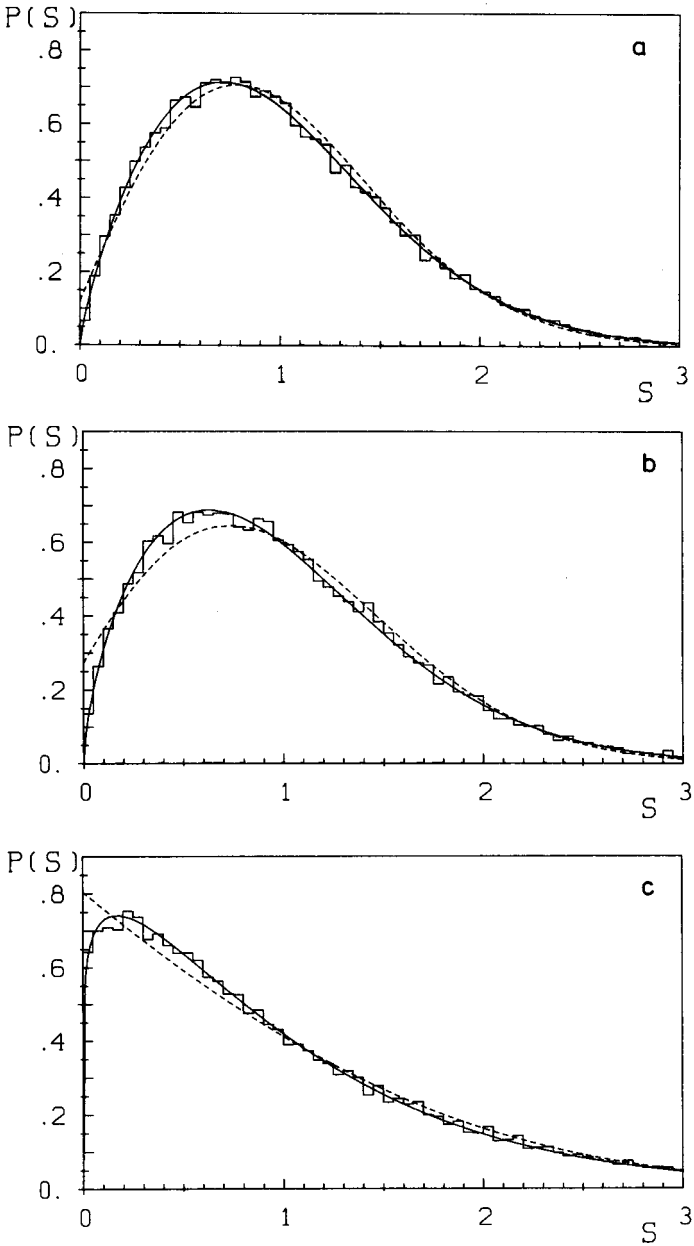

Fig. 8. Level spacing distribution of the orthogonal kicked top obtained from 300 matrices with $p \approx 1.3$ and $j = 100, \ldots, 119$. Solid lines represent the Brody distribution and dashed lines the Berry–Robnik distribution. Kicking strength a) $k = 4.0$, b) $k = 3.0$, and c) $k = 2.5$.

with $B(q) = \{\Gamma[(2+q)/(1+q)]\}^{1+q}$, represented in Figure 8 by solid lines,

provides much better approximation to the level spacing distribution of the kicked top. Best fit Histogram in Fig. 8.a, obtained for $k = 4.0$, gives the Brody parameter $b = 0.79$. The average squared deviation per bin χ^2/ν is equal to 0.9 (in comparison to 4.1 for best fit of the Berry–Robnik distribution), what gives a remarkable confidence level of the χ^2 test of order of 50%. For smaller values of the kick strength ($k = 3.0$ in Fig. 8.b and $k = 2.5$ in Fig. 8.c) the quality of fit with the Brody distribution is not as good (confidence level of order of 5%), but still better than with the Berry–Robnik distribution. However for nearly regular classical dynamics ($k \sim 1.5$) and a Poisson-like spectrum, the latter distribution is more accurate. The level spacing distribution (88) gives overall similar quality of fit as the Brody distribution. For all distributions considered the fitting parameter increases slightly with the quantum number j.

In spite of the fact that physical arguments suggest to apply the Berry–-Robnik distribution for a dynamical system with a mixed dynamics [125], the simple Brody formula appears to be more useful for the quantized kicked top. We have thus confirmed numerous earlier observations [123, 128, 210] concerning an applicability of the Brody distribution for quantum systems displaying a transition from regular to chaotic dynamics. On the other hand, it seems that there exists no universal features of the transition between Poisson and orthogonal ensemble, and for different dynamical systems different ensembles of random matrices are appropriate.

Parallel to the study of level distribution we analyzed the distribution of eigenvector components. Figure 9 presents the eigenvector statistics in a logarithmic scale for similar samples of data obtained for $j = 100, \ldots, 119$ and 17 values of $p \sim 1.3$. For $k = 5.0$ the corresponding classical system is entirely chaotic, $r = 1$ and the eigenvector statistics $P(y)$ is well described by the Porter–Thomas distribution, represented in Figure 9.a by a dashed line. In order to make easier a direct comparison of results obtained for various values of j we used the normalization $\langle y \rangle = 1$. With decreasing values of the kicking strength ($k = 3.5$ in Fig. 9.b and $k = 2.5$ in Fig. 9.c), the distribution of eigenvectors components becomes broader. The quantitative character of the eigenvector statistics is reproduced by the χ^2_β distribution (5) with $0 < \beta < 1$. Since this distribution is not capable to describe the highest peak of the histogram, moving right with decreasing kick strength, we have resigned to use it to fit the numerical data. Moreover, the distribution (21) of additive random matrices, presented in Fig. 3, definitely fails to describe numerical data of the kicked top.

The family of interpolating distributions recently constructed for eigenvector statistics of band random matrices [120] correctly describes only essential features of the numerical data: for small values of k the histogram becomes flat (in the logarithmic scale) and tends to the appropriately nor-

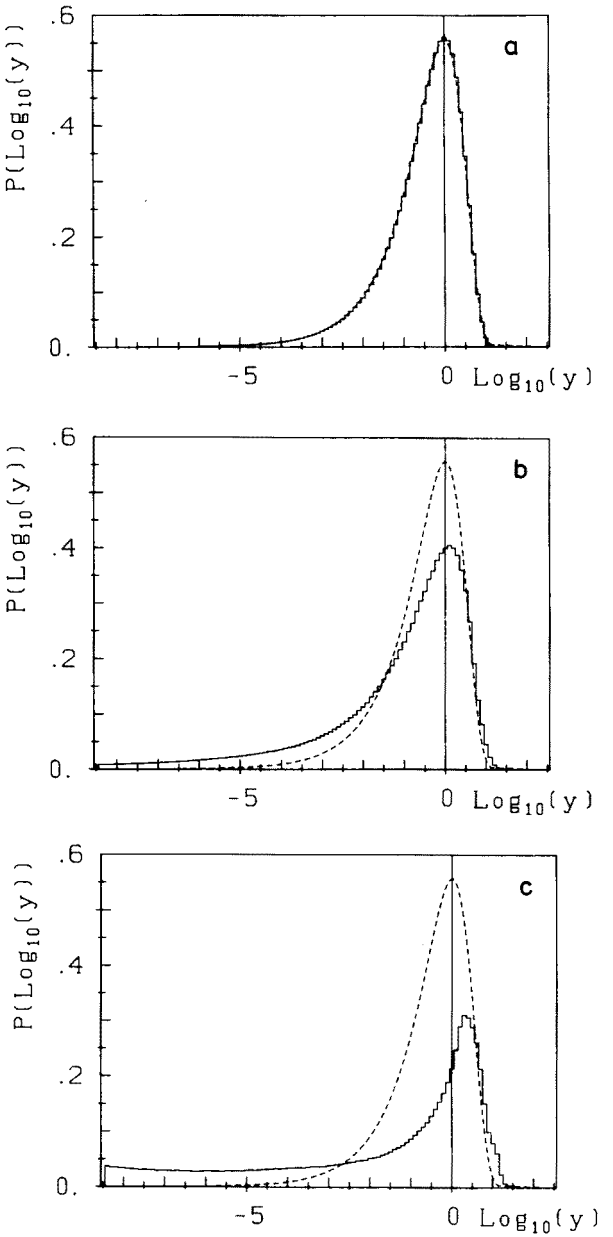

Fig. 9. Eigenvector statistics of the orthogonal kicked top for $p = 1.3$ and a) $k = 5.0$, b) $k = 3.5$, and c) $k = 2.5$. Dashed line denotes the Porter–Thomas distribution typical of orthogonal ensemble.

malized $1/y$ distribution. It is worth to stress that the peaks of the eigenvector statistics, visible in Fig. 9.b and 9.c, are not universal but depend on

the choice of basis used to represent eigenvectors [136].

All the parameters characterizing the transition from order to chaos in classical version of the kicked top with $p = 1.3$ and the transition from Poisson to orthogonal ensemble for the corresponding quantum model are collected in Table I.

TABLE I

Parameters characterizing changes of the dynamics of the orthogonal kicked top (55) with varying kick strength k. Classical system is described by the ratio r of the phase space covered by chaotic layers and the mean Lapunov exponent Λ computed outside islands of stability. Eigenvectors of the corresponding quantum system ($j = 100$) are portrayed by the mean entropy γ and by the mean localization length η. Spectrum is characterized by the best fit values of the Brody distribution q, and of the Berry–Robnik distribution b. The average squared deviation per bin χ^2/ν describes the quality of each fit.

kick strength	Classical system		Quantum system					
			Eigenvectors		Eigenvalues			
k	r	Λ	γ	η	q	χ^2/ν	b	χ^2/ν
1.0	0.00	–	0.67	0.28	0.05	1.3	0.22	1.9
2.0	0.06	0.07	0.81	0.48	0.06	1.2	0.33	1.1
2.5	0.77	0.21	0.85	0.57	0.14	0.9	0.44	2.4
3.0	0.88	0.34	0.92	0.74	0.37	2.0	0.67	4.7
3.5	0.96	0.47	0.97	0.90	0.64	1.3	0.85	6.0
4.0	0.99	0.61	0.99	0.96	0.79	0.9	0.94	4.1
4.5	1.00	0.73	1.00	1.00	0.93	1.4	0.98	3.0
5.0	1.00	0.84	1.00	1.00	0.98	1.1	0.99	1.2

4.3. Eigenvector statistics in rotated basis

Entropy of eigenvectors, used to characterize the quantized model of the kicked top and displayed in Fig. 7, is calculated in the eigenbasis of the unperturbed system. In order to analyze, to what extend the choice of basis determines the properties of eigenvectors, we computed the eigenvector components in rotated basis (22). The average overlap of the eigenstate $|\psi_i(k_1)\rangle$ of the operator $\widehat{F}_o(k_1, p)$ with an eigenstate $|\psi_n(k_1 + \Delta k\rangle$ of the operator $\widehat{F}_o(k_1 + \Delta k, p)$ is measured by the mean entropy $\gamma = \langle H_{\Delta k}\rangle / \bar{H}_1$ defined in (8) and (9). Figure 10 presents the entropy in rotated basis plotted in a log-log scale against the rotation parameter Δk for $j = 50$ and $p = 1.3$. Results obtained in the regime of classically chaotic motion for $k_1 = 9.0$ ($\star$) and for $k_1 = 6.0$ ($\triangle$) are similar. For small values of the rotation parameter, the entropy displays a quadratic growth with Δk. For a critical value Δ_c, of order of 10^{-1}, the entropy saturates and tends to

the value $\bar{H}_1$, typical of the orthogonal ensemble ($\gamma = 1$). It means that for the classically chaotic system, the eigenvector statistics agrees with the Porter–Thomas distribution, provided the basis is rotated by a parameter Δk larger than Δ_c. Analyzing the model of quantum kicked top for several values of the quantum number j, we have observed that the critical rotation parameter Δ_c is proportional to j^{-1}. For smaller values of the kick strength $k_1 = 3.0$ (+) and $k_1 = 0$ (o) the COE limit is achieved for values of Δk much larger than Δ_c. The value $k_2 = k_1 + \Delta k$ is than so large that the classical dynamics for the kick strength k_2 is chaotic.

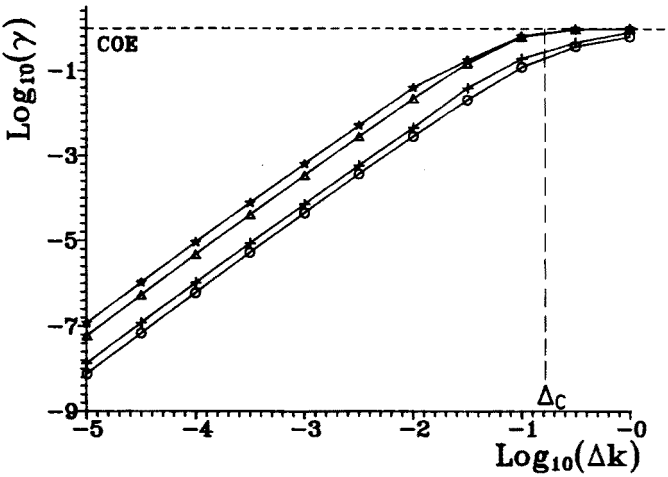

Fig. 10. Mean entropy γ of eigenvectors of operator $\widehat{F}_1$ represented in a rotated basis depicted against the rotation parameter Δk in a log-log scale. Parameter p set to 1.3, while the kicking strength $k_1 = 9.0$ ($\star$), $k_1 = 6.0$($\triangle$), $k_1 = 3.0$ (+), $k_1 = 1.0$($\bigcirc$).

It means, therefore, that each eigenvector statistics, carries not an absolute piece of information about a single dynamical system, but rather, about two systems described by Hamilton operators determining two orthonormal basis. Figure 11 shows the dependence of the mean entropy of eigenvectors of the system $\widehat{F}_1 = F_o(k_1, p)$ calculated in the eigenbasis of $\widehat{F}_2 = F_o(k_2, p)$ on the parameter k_1. Results obtained for $k_2 = 0.0$, represented by circles in the figure, reflect the transition from Poisson–COE, as in the figure 7.a. The increase of the entropy γ to unity at $k_1 \sim 3.5$ corresponds in this case to the transition from regular to chaotic dynamics in the classical model. Results obtained for other values of the parameter k_2, which defines the basis used to expand the eigenvectors, have a different character. In each case: $k_2 = 2.0$ ($\triangle$), $k_2 = 4.0$ ($\times$), and $k_2 = 6.0$ ($\star$) the entropy exhibits dips

at $k_1 \sim k_2$. Small values of the entropy in such circumstances cannot be associated with the regular dynamics of the corresponding classical system, but exclusively with the choice of basis used to represent the eigenvectors of the quantum system.

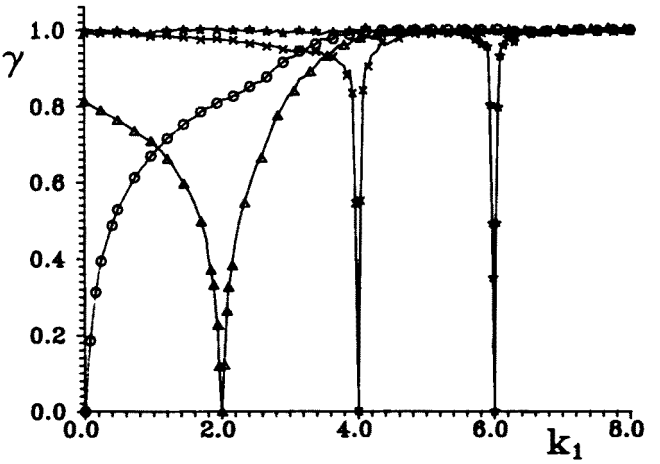

Fig. 11. Dependence of mean entropy γ of eigenvectors of on the kicking strength k_1. The value k_2 defining the basis used to represent the eigenvectors of $\widehat{F}_1(k_1)$ is equal to $k_2 = 0.0$ (○), $k_2 = 2.0$(△), $k_2 = 4.0$ (×), $k_2 = 6.0$(⋆).

A complementary information might be obtained by studying the eigenvector statistics $P(y)$ in an rotated basis. We have fixed the values of the kicking strength k of the orthogonal top $F_o(k,p)$ and used changes of the parameter p to achieve the "rotation" of the basis. Figure 12 presents the eigenvector statistics obtained for $j = 100$, $p_1 = 1.7$ and various values of the kicking strength k and the rotation parameter Δp. Histograms 12.a, 12.b, and 12.c show the statistics of a classically chaotic system ($k = 9.0$). In the case of the rotation parameter $\Delta p = 0.1$, which exceeds the critical value Δ_c, the eigenvector statistics complies to the Porter–Thomas distribution, represented by dashed line. For smaller values of Δp the main peak of the distribution is shifted toward smaller values of y (see Fig. 12.b and 12.c). The position of the center of this peak y_m depends on the rotation parameter as $y_m \sim (\Delta p)^2$. Moreover, a peak at $y \sim \log_{10}(j)$ appears, which corresponds to the diagonal elements of the matrix containing eigenvectors. This features of the distribution of eigenvectors of the Floquet operator F_o in the rotated basis resemble the distribution (21) of the additive random matrices. However, a better approximation to the histogram is obtained by using the $\chi^2_{\beta,\langle y\rangle}$ distribution (5) with $\beta = 1$ and the mean value $\xi = \langle y\rangle$ treated as a free parameter

$$P(y) = \frac{N-1}{N-\xi}\chi^2_{\beta,\xi} + \frac{1-\xi}{N-\xi}\delta(y-N)\,. \tag{61}$$

The size of the matrix N is equal to j or $j+1$, depending on the parity class considered. The first term of the distribution (61) represents small, off-diagonal elements of the eigenvectors matrix, while the second term describes N diagonal elements with the module close to unity. Coefficients standing before both terms are determined by the normalization condition. Best fit of the mean value ξ in (61) for different values of the quantum number j and the rotation parameter Δp gives a simple formula

$$\xi = \frac{C_p}{(j\Delta p)^2}\,, \tag{62}$$

where the proportionality constant $C_p \approx 5.3$. For the Porter–Thomas distribution, typical of orthogonal ensemble, the mean value of the eigenvector component is set to unity, $\langle y \rangle = 1$. Making use of the above relation we may estimate the value of the minimal rotation parameter $\Delta_c p$ producing a *random basis*, in which the eigenvector statistics conforms to the predictions of random matrices:

$$\Delta_c p = \frac{\sqrt{C_p}}{j}\,, \tag{63}$$

with a constant $\sqrt{C_p} \approx 2.3$. A similar relation holds also for the rotation of the Floquet operator $\widehat{F}_o(p,k)$ along the k axis, with a fixed value of p. If the difference of the kick strength $k_1 - k_2$ is greater than $\Delta_c k \approx 8.5/j$, the eigenvector statistics is described by the Porter–Thomas distribution, provided the classical system $\widehat{F}_o(p,k_1)$ is chaotic.

Histograms 12.d–12.f present the eigenvector statistics for the mixed system, $k = 3.0$ with the rotation parameter Δp equal to 10^{-1}, 10^{-3} and 10^{-4}, respectively. Note the change of the vertical scale, compared to the upper figure. In the case 12.d the rotation parameter is so large that the distribution $P(y)$ is similar to the eigenvector statistics in the unperturbed case, presented in Fig. 9. The solid line represents the χ^2_β distribution (5). The best fit of the parameter $\beta \approx 0.41$ might be used to characterize the results obtained. The shift of the main peak of the distribution occurring for smaller values of the rotation parameter Δp and displayed in Figures 12.e and 12.f, is also governed by the formula (62). A slightly generalized distribution (61) (with a real number $\beta \in (0,1)$), might be used therefore as a first approximation of the distribution of eigenvector components in rotated basis. For the case presented in Fig. 12.e ($\Delta p = 10^{-3}$) the best fit of (61) gives $\xi = 10^{-3.3}$ and $\beta = 0.34$, while for the histogram 12.f $\xi = 10^{-5.3}$ and $\beta = 0.33$.

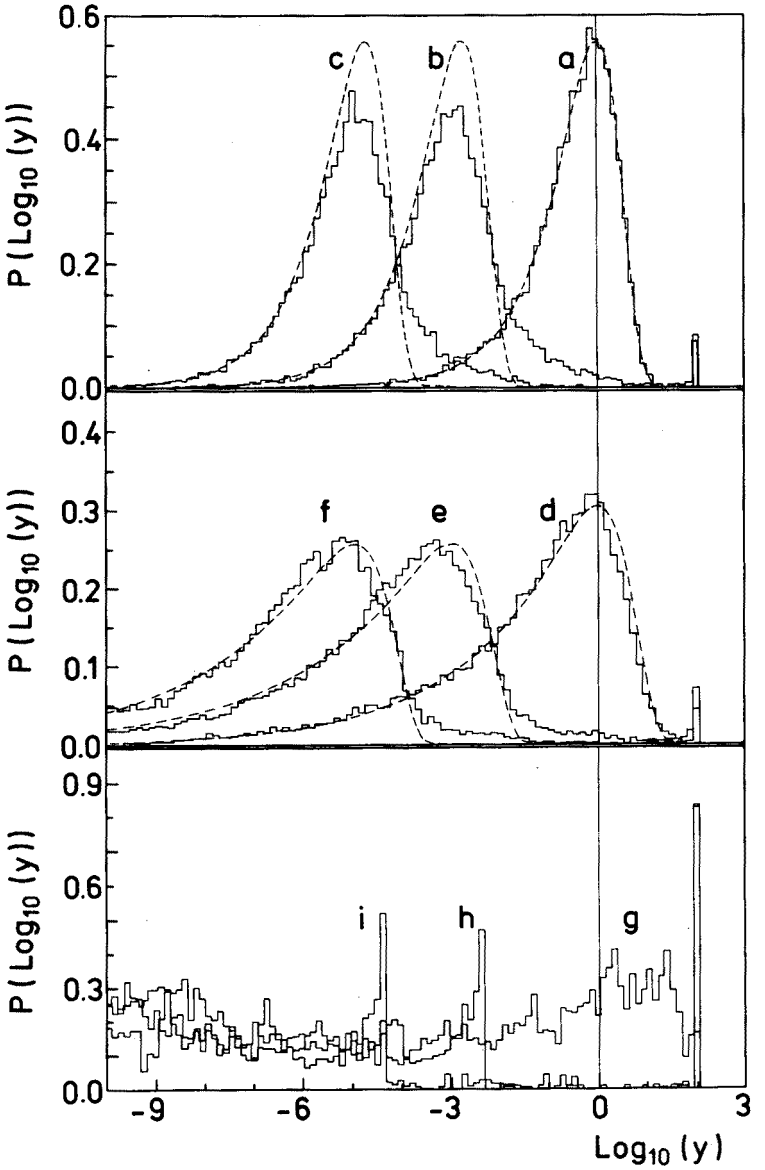

Fig. 12. Eigenvector statistics of the kicked top with $p = 1.7$ in rotated basis. Histograms **a-c** obtained in classically chaotic regime ($k = 9.0$), histograms **d-f** obtained for classically mixed phase space ($k = 3.0$), and **g-i** obtained for classically regular dynamics ($k = 1.0$). Rotation parameter Δp is equal to 10^{-1} for **a**, **d**, **g**; $\Delta p = 10^{-3}$ for **b**, **e**, **h**, and $\Delta p = 10^{-4}$ for **c**, **f**, **i**. Note the change of scale on vertical axis.

Data presented in Figs 12.h–12.i are obtained for small kicking strength $k = 1$, for which regular dynamics dominates in the classical phase space. Histogram obtained for sufficiently large rotation parameter $\Delta p = 10^{-1}$ and displayed in Fig. 12.h, is flat (in the logarithmic scale), what agrees to the χ^2_β distribution with $\beta \to 0$. In a full analogy with the both cases discussed before, for smaller values of Δp the main peak of the distribution is shifted toward smaller values of y, what is compensated by an appearance of a singularity at $y = N$, connected to diagonal elements of the eigenvector matrix.

As follows from results presented in Fig. 11, a small value of the mean entropy of eigenvectors of given quantum system, $\gamma \ll 1$, may be interpreted as a fingerprint of classically regular dynamics. However, equally legitimate is an interpretation that the basis used to represent the eigenvectors is close to the eigenbasis of the system. Taking into account exclusively the mean entropy of the eigenvectors it is thus impossible to figure out, which of these two possibilities is the right one. Results shown in Figure 12 demonstrate that this ambiguousness might be clarified by studying the nature of the eigenvector statistics.

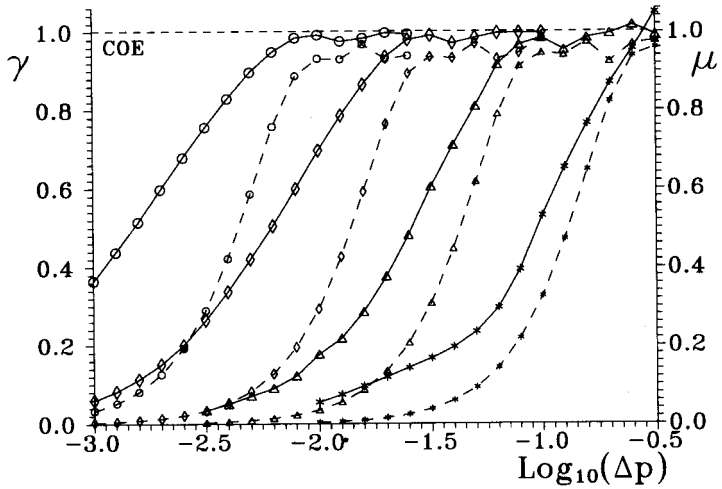

Fig. 13. Entropy of eigenvectors γ plotted against rotation parameter Δp for $k = 11.0$, $p = 1.4$ and $j = 316(\bigcirc)$, $j = 100(\diamond)$, $j = 32(\triangle)$, $j = 10(\star)$. Numerical data joined by solid lines. Corresponding smaller symbols, joined by dashed lines, represent values of the coefficient μ defined by (65).

In order to portray the changes of the minimal rotation parameter $\Delta_c p$ with j, we analyzed the dependence of the entropy of eigenvectors γ on the rotation parameter and observed, for which values of Δp the entropy

achieves the COE value. Solid lines in Fig. 13 present the dependence of entropy on the rotation parameter (in a logarithmic scale) for $j = 10, 32, 100,$ and 316. These values of j form a geometric sequence and in the logarithmic scale the distance between subsequent numbers is approximately 0.5. Observe, that four solid lines in Fig. 13 have a similar behaviour and might be put into a single curve by an appropriate shift along the horizontal axis by a multiplicity of 0.5. This fact confirms the relation (63), which estimates the value of Δp sufficient to assure the COE-like properties of eigenvectors.

Comparable conclusions might be drawn from a complementary and more general reasoning. The statistics of components of eigenvectors of a unitary operator $\widehat{F}_1$, represented in the eigenbasis of $\widehat{F}_2$, complies to the predictions of random matrices, provided both operators do not commute and theirs eigenbasis are sufficiently different. To describe this difference quantitatively we calculate squared norm of the commutator

$$\| [F_1, F_2] \|^2 = 2\big(N - \langle F_2 | F_1^\dagger F_2 F_1 \rangle\big) , \tag{64}$$

where N is the size of the matrix representation of the both operators. The degree of commutativity between $\widehat{F}_1$ and $\widehat{F}_2$ might be characterized by a coefficient

$$\mu = 1 - \mathrm{Re}\big(\mathrm{Tr}(F_2^\dagger F_1^\dagger F_2 F_1)\big)/N . \tag{65}$$

Trace in the above definition is equivalent to the scalar product $\langle F_2 | F_2' \rangle = \langle F_1' | F_1 \rangle$, where in an analogy to (33) we denote $F_2' = F_1^\dagger F_2 F_1$ and $F_1' = F_2^\dagger F_1 F_2$. The coefficient μ is equal to zero for $F_1 = F_2$ and tends to unity for orthogonal operators satisfying $\langle F_1 | F_2 \rangle = 0$. The values of μ, obtained for the orthogonal top with the same values of j, are represented in Fig. 13 by smaller corresponding symbols joined by dashed lines. There is no reason to expect that for a given spin length j the values of γ and μ would be equal. However, the sudden growth of the coefficient μ coincides, for any j, with the minimal value of the rotation parameter Δp, for which the entropy tends to the COE value. Also in the other case, for which the rotation of the basis is achieved by a variation of the kicking strength $k_2 = k_1 + \Delta k$, the dependencies $\gamma(\Delta k)$ and $\mu(\Delta k)$ are correlated and display behaviour similar to this presented in Fig. 13. The condition

$$\mathrm{Re}\big(\langle \widehat{F}_1 | \widehat{F}_1' \rangle\big) \ll N , \tag{66}$$

might be thus considered as a simple criterion allowing to select a *random basis*, in which the eigenvector statistics complies with the predictions of canonical ensembles of random matrices. Note a similarity between the definition (34) of an operator (Hermitian observable) $\widehat{B}$ random with respect

to the system $\widehat{F}_2$ and the concept of a random basis, determined by a unitary operator $\widehat{F}_1$.

For the considered model of orthogonal top (55) with $\widehat{F}_1 = \widehat{F}_o(k, p_1)$ and $\widehat{F}_2 = \widehat{F}_o(k, p_1 + \Delta p)$ the trace in equation (65) is taken of the operator $\widehat{O} = \widehat{F}_o(-k, -\Delta p) * \widehat{F}_o(k, \Delta p)$. The trace $\mathrm{Tr}(\widehat{O})$ equals N for $\Delta p = 0$, decreases with growing rotation parameter, roughly speaking, as $\sum_{m=-j}^{j} \exp(im\Delta p)$ and tends to zero for $\Delta_c p \approx \pi/2j$. This simple approximation suits well the observed relation (63). The condition (66), or in the specific case of the kicked top, the relation (63), might be used to check the statistical independence of spectra collected together in order to increase the statistics. To prepare level distribution shown in Fig. 8 we put together data of several systems $F_o(p, k)$ with fixed k, the spin length $j \approx 100$, and the parameter p varying by the step comparable to the minimal rotation $\Delta_c p$.

4.4. Transition orthogonal–unitary

Orthogonal top, defined by the operator (55), possesses the antiunitary symmetry (58). This symmetry might be broken by an additional unitary factor $\exp(idJ_y^2/2j)$. Modified Floquet operator

$$\widehat{F}_u = \exp\left(\frac{-id\widehat{J}_y^2}{2j}\right) \exp\left(\frac{-ik\widehat{J}_x^2}{2j}\right) \exp(-ip\widehat{J}_z)\,, \tag{67}$$

corresponds to an Hamiltonian, analogous to (52), with two subsequent kicks, governed by operators $\widehat{J}_y^2$ and $\widehat{J}_x^2$. Such system does not have any antiunitary symmetry and for sufficiently large values of the parameter d operator $\widehat{F}_u$ can be described by circular unitary ensemble [15], provided $k \neq d$.

By increasing value of the parameter d in (67) one may therefore investigate the transition COE–CUE. It has been shown [113] that the level spacing distribution during this transition is well approximated by the formula (19), obtained for the additive random matrices. However, the fitting parameter λ_f, which enters formula (19) and describes the speed of transition between circular orthogonal and unitary ensembles, scales as [134]

$$\lambda_f = j^{3/2} d^2\,. \tag{68}$$

This behavior differs the transition between Gaussian ensembles of Hermitian matrices from corresponding transition between circular ensembles of unitary matrices.

The statistics of the eigenvector components in the intermediate case might be approximated by the χ_β^2 distribution with $\beta \in (1, 2)$. It has been demonstrated [133] that the distribution

$$P_b(y) = \frac{b \exp\left(-\frac{yb^2}{4(b-1)}\right)}{2\sqrt{b-1}} I_o\left(\frac{y\ b\ (2-b)}{4\ (b-1)}\right), \quad b \in (1,2) \tag{69}$$

provides much better fit to the numerical data. In the above formula I_o denotes the Bessel function of order zero. When b varies between 1 and 2 the distribution (69) is transformed from the $\chi^2_{\beta=1}$ distribution (OE) to the $\chi^2_{\beta=2}$ distribution (UE). The transition of the properties of eigenvector statistics and the entropy of eigenvectors is controlled [134] by a scaling parameter

$$\lambda_w = jd^2 . \tag{70}$$

During the transition between COE and CUE controlled by increase of the parameter d the changes of the properties of the eigenvectors, characterized by (70), occur faster than the changes of the properties of the spectrum governed by (68). It means therefore that neither the additive model of Hermitian matrices (4), nor the Dyson model of Brownian motion in space of random unitary matrices [19], is capable of describing correctly the transition between orthogonal and unitary ensemble occurring in this exemplary dynamical system.

Note that by a rotation procedure the matrix F_1, representing the orthogonal top (55), might be transformed into a symmetric form. Taking for the unitary matrix $U = \exp(ipJ_z/2)$ and defining $F'_o := U^\dagger F_o U$ we get a symmetric matrix $F'_o = F'^T_o$ with the same spectrum as F_o. Squared matrix U^2 is just equal to the second unitary factor of (55). Alternatively, one may take for U another matrix $\exp(-ikJ_x^2/4j)$, which is correlated with the first factor of the orthogonal top. Since the unitary top (63) consists of three different unitary factors, such technique is not applicable any more. The only symmetric matrix representation of the operator $\widehat{F}_u$ is therefore diagonal.

It is possible to symmetrize matrix F_u in an artificial way and define a symmetric matrix

$$W_1 = F_u F_u^T . \tag{71}$$

Matrix W_1 represents a periodical dynamical system composed of four kicks

$$\widehat{W}_1 = \exp\left(\frac{-id\widehat{J}_y^2}{2j}\right) \exp\left(\frac{-ik\widehat{J}_x^2}{2j}\right) \exp(-i2p\widehat{J}_z)$$
$$\times \exp\left(\frac{-ik\widehat{J}_x^2}{2j}\right) \exp\left(\frac{-id\widehat{J}_y^2}{2j}\right) . \tag{72}$$

Figure 14 represents the level spacing distribution of 400 matrices W_1 with parameter k varying from 10 to 14. Parameters p and d are chosen in

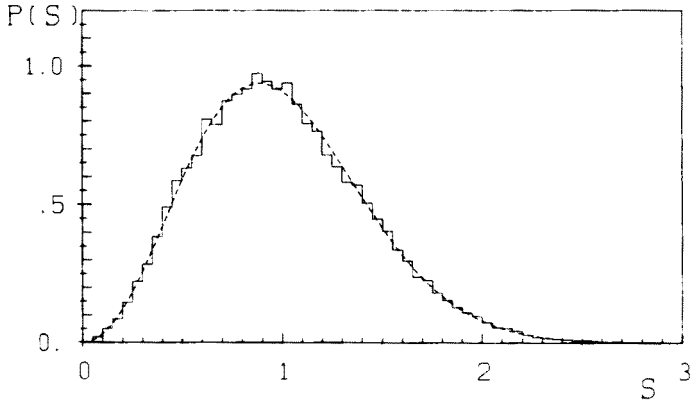

Fig. 14. Level spacing distribution cumulated of 400 matrices $W_1 = F_u * F_u^T$. Matrices representing unitary top $\widehat{F}_u$ for $p = 1.0, d = 5.0, k \in (10.0, 14.0)$ belong to CUE, while spacing distribution of matrices W_1 agrees with the COE distribution represented by solid line.

such a way that matrices F_u have the properties typical to CUE. On the other hand, as may be seen in the figure, the level statistics of symmetric matrices W_1 coincides with the exact COE distribution [18, 211] represented by a solid line. The χ^2 test gives an acceptable confidence level of 20%, in contrast to 10^{-9} obtained for the Wigner surmise (2). In addition, the mean entropy of eigenvectors agrees to a remarkable accuracy with the value resulting from formula (9) for $\beta = 1$. Also other unitary matrices composed of several unitary factors F_i in a way analogous to (72):

$$U = F_1 F_2 \cdots F_n \cdots F_2 F_1 \tag{73}$$

possesses, for generic values of the parameters, the properties of COE.

Furthermore, it is interesting to analyze products of two unitary matrices, which represent the orthogonal top $\widehat{F}_o$ and pertain to COE. Operator

$$\widehat{W}_2 = \exp\left(\frac{-ik_1\widehat{J}_x^2}{2j}\right)\exp(-ip_1\widehat{J}_z)\exp\left(\frac{-ik_2\widehat{J}_x^2}{2j}\right)\exp(-ip_2\widehat{J}_z), \tag{74}$$

represents a dynamical system governed by two kicks of different strength within a period $p_1 + p_2$. We denote the differences in parameters by $\Delta k = k_2 - k_1$ and $\Delta p = p_2 - p_1$. For $\Delta p = \Delta k = 0$ the matrix W_2 is equal to F_o^2 and, due to overlapping of the eigenvalues of F_o from the interval $(0, \pi)$ with these from the interval $(\pi, 2\pi)$, the statistical properties of the spectrum of W_2 differ significantly from these characteristic of COE. In a rough approximation the level spacing distribution of W_2 might be described

by a particular form of the Berry–Robnik distribution [125] constructed by superimposing two Wigner-like spectra and appropriate to describe the case of two distinct chaotic domains in the classical phase space.

Let us keep one of the differences (Δk or Δp) equal to zero and allow one the other one to take non-zero values. The matrix W_2 can be then transformed by a unitary rotation into a matrix $W_2' = U^\dagger W_2 U$ of the form (73). For example if $\Delta k = 0$ we take $U = \exp(ip_2 J_z/2)$ and get a symmetric form

$$W_2' = \exp\left(\frac{-ip_2 J_z}{2}\right) \exp\left(\frac{-ikJ_x^2}{2j}\right) \exp(-ip_1 J_z) \times \exp\left(\frac{-ikJ_x^2}{2j}\right) \exp\left(\frac{-ip_2 J_z}{2}\right). \tag{75}$$

Numerical investigation showed that for sufficiently large values of the difference Δp (or Δk), the matrix W_2 has in this case the COE spectrum.

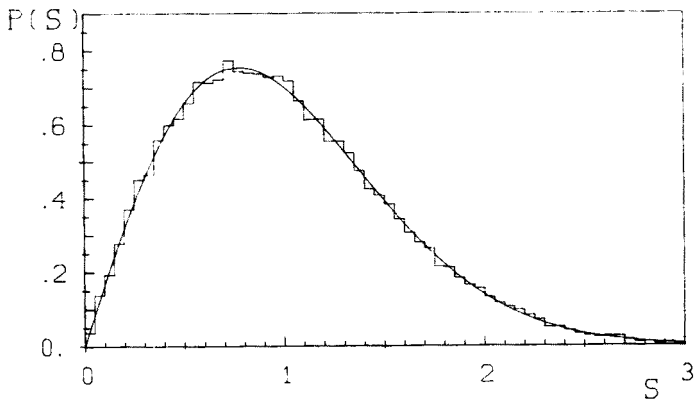

Fig. 15. Level spacing distribution cumulated of 500 matrices $W_2 = F_o(k_1, p_1) * F_o(k_2, p_2)$. Matrices representing orthogonal top $\widehat{F}_o$ for $p_1 = 1.7, p_2 = 2.3, k_1 \in (8.0, 13.0)$, and $k_2 = k_1 + 4.0$ belong to COE, while spacing distribution of matrices W_2 conforms to the CUE distribution represented by dashed line.

If both differences are not equal to zero the matrix W_2 cannot be transformed into the form defined by (73). Figure 15 shows the level statistics made of 500 matrices W_2 with $p_1 = 1.7$, parameter k_1 varying from 8.0 to 13.0, the differences $\Delta p = 0.03$ and $\Delta k = 0.2$. In this case the numerical data fit well to the spacing distribution of CUE, represented by a dashed line. Moreover, the mean entropy of eigenvectors is close to the value characteristic of the unitary ensemble. Values of the differences Δp and Δk necessary to assure that W_2 has properties typical of CUE, depend on j

and are of the order of the minimal rotation parameters $\Delta_c p$ and $\Delta_c k$, respectively. Keeping the parameter Δp constant and increasing the difference Δk one can study the transition COE–CUE in an alternative way.

Analyzing a quantum system described by a N-dimensional matrix S one usually looks for a unitary matrix U_0, such that $D_0 = U_0^\dagger S U_0$ is diagonal, and examines the correlations between diagonal elements of D_0 (spectrum) or the statistics of the elements of U_0 (eigenvectors). Each column of the unitary matrix U_0 (eigenvector of S) has an arbitrary phase, since for any diagonal unitary matrix D_a the matrix $U_0' := D_a U_0$ diagonalizes also the matrix S. In spite of this ambiguousness we found it interesting to analyze the properties of an exemplary matrix U_0 and to diagonalize it obtaining $D_1 = U_1^\dagger U_0 U_1$. Diagonalizing the resulting unitary matrix of eigenvectors U_1 we define the diagonal matrix $D_2 = U_2^\dagger U_1 U_2$ and, by repeating this procedure further on, the diagonal matrices $D_{l+1} = U_{l+1}^\dagger U_l U_{l+1}$, $l = 1, 2, \ldots,$.

Taking the for the initial matrix S the matrix F_u, representing the unitary top (67) and possessing the CUE properties, we noticed that the matrix of eigenvectors U_0 displays also the spectrum typical of the unitary ensemble (independently of the choice of N arbitrary phases of eigenvectors). In addition, the mean entropy of eigenvectors constructing the matrix U_1 is identical with the mean entropy of the eigenvectors of F_u collected in U_0. The same observations hold for other matrices of the sequence $U_1, U_2 \ldots$. Interestingly, the same properties has the sequence of matrices U_l, $l = 1, 2, \ldots$, generated from the matrix (67) with arbitrary values of the parameter d (including $d = 0$, for which F_u pertains to the orthogonal ensemble). Further numerical experiments suggest that for sufficiently large number l depending on a given non-diagonal unitary matrix U_0 any matrix of the sequence $\{U_l, U_{l+1}, U_{l+2}, \ldots\}$ has the properties of CUE.

5. Concluding remarks

We have analyzed two models of random matrices which interpolate between canonical ensembles: I) — band random matrices, parametrized by the band width b, and II) — additive random matrices, described by the perturbation parameter λ. Both ensembles display the property of scaling. For real, N-dimensional band matrices the scaling variable is $x = b^2/N$, for the properties of spectrum [118], as well as for eigenvectors [116, 120]. We have demonstrated that the same scaling law holds also for the model of complex band matrices which interpolate between Poisson, orthogonal, and unitary ensembles.

For additive random matrices the velocity of changes in the spectral properties is proportional to $\lambda\sqrt{N}$, where the proportionality constant is different for the wings of the spectrum and its center [114]. For this model

the scaling law governing the eigenvector statistics is different from the scaling relation for the spectrum. The distribution of eigenvector components $P(y)$ can be characterized by the average Shannon entropy of eigenvectors $\langle H \rangle$ or the closely related localization length η.

Eigenvector statistics of real random matrices in the GOE regime ($b^2/N \gg 1$ or $\lambda \gg 1$), calculated in the basis in which the matrix was constructed, is given by the Porter–Thomas distribution and the Shannon entropy complies with predictions of the orthogonal ensemble. On the other hand, for an inappropriate choice of basis (for example, in the additive model, too small a value of the rotation parameter $\Delta\lambda$ determining the closeness to the eigenbasis of the matrix), the eigenvector distribution of this matrix looks similar to the eigenvector distribution of a Poisson-like matrix ($\lambda \ll 1$).

Quantized dynamical systems corresponding to classically chaotic motion might be described by canonical ensembles of random matrices: Gaussian for the autonomous systems, and circular for time-dependent, periodical systems. The choice of one of the three universality classes depends on the symmetry of the system. Properties of spectra characterized by the level spacing distribution $P(s)$ or the spectral rigidity $\Delta_3(L)$ and the number variance $\Sigma^2(L)$ (for short range L) are universal for all quantum systems (with restrictions to systems, for which the dynamical localization occurs). On the other hand, the properties of eigenvectors are universal provided the unitary operator $\widehat{F}_1$ representing a periodical quantum system is represented in an appropriate basis. We call the eigenbasis of a unitary operator $\widehat{F}_2$ *random with respect to the system* $\widehat{F}_1$, if $\mathrm{Re}(\langle \widehat{F}_2 | \widehat{F}_1^{\dagger} \widehat{F}_2 \widehat{F}_1 \rangle) \ll N$. We conjecture that the statistics of components of eigenvectors of a classically chaotic system, represented in a random basis, agrees with the prediction of random matrices. This approach might be also generalized for Hermitian matrices representing autonomous quantum systems.

The model of the periodically kicked top provides an efficient tool allowing us to construct unitary matrices typical of circular ensembles. We investigated some of their algebraic properties. A product of two different matrices typical of COE possesses the properties of CUE. Moreover, a product of UU^T, where U pertains to CUE, displays all features of a COE matrix. An arbitrary matrix U_1 diagonalizing any CUE-like matrix U_0 has the properties of CUE. The same concerns a matrix U_{l+1}, selected from the set of all matrices diagonalizing the matrix U_l. It seems therefore that the set of matrices with the CUE properties is invariant under the operation of diagonalization.

Periodically kicked top is also useful to simulate transitions between circular ensembles of random matrices. The transition from Poisson to orthogonal ensembles corresponds to the classical transition from regular motion.

The Berry–Robnik distribution, invented for such a case [125], approximates the level spacing distribution obtained numerically less accurately than the Brody distribution, created *ad hoc* [17]. Some aspects of this transition (the character of the level spacing distribution and the eigenvector statistics, the same scaling law for eigenvalues and eigenvectors) might be associated with the model of band random matrices. On the other hand, some aspects of the transition between orthogonal and unitary ensembles corresponding to a process of the time-reversal symmetry breaking and realized by the unitary kicked top (67), may by linked with the model of additive random matrices. This model is known to be useful to represent some basic features of singular billiards [72, 140] or other pseudointegrable systems [141]. It is difficult therefore, to demonstrate a superiority of one of the models of random matrices as regards a possibility to describe parametric dynamics of quantum system. The transitions inside a given canonical ensemble of random matrices possess some universal features [102, 109]. On the other hand, it is rather dubious that also the transitions between ensembles have universal nature and one might, for example, discover a level spacing distribution, interpolating between Poisson and Wigner distributions, applicable to all quantized dynamical systems. One may try however, to specify a particular class of dynamical systems, for which the transitions between ensembles have a common nature, and find an appropriate model of random matrices. Further work is needed to verify this possibility.

There exist simple rules allowing us to construct numerically a Hermitian matrix belonging to one of the Gaussian ensembles [17]. Discussed models of random matrices consist of Hermitian matrices and are suitable to describe autonomous systems. Properties of time-dependent, periodical systems, are described by the circular ensembles of unitary matrices. Because of the correlations between the elements assuring unitarity, creating a matrix pertaining to one of the circular ensembles by means of a random numbers generator is more difficult. In order to ensure a closer connection to quantum periodical systems it is therefore important to solve this problem and to define ensembles of unitary matrices interpolating between canonical circular ensembles. In context of the recent results revealing unexpected scaling variable describing the transition COE–CUE in the kicked top [134] it would be also interesting to compare the properties of the transitions between Hermitian matrices belonging to the Gaussian ensembles and unitary matrices of the corresponding circular ensembles.

Each eigenstate of a quantum system, described by a matrix of size N, may be represented by a set of precisely N zeros of the Husimi distribution of the state considered [131, 206, 212, 213]. Character of the distribution of N^2 zeros in the phase space has been linked to the behaviour of the corresponding classical system. Parametric dynamics of a quantum system

could be in this way described by studying the motion of the zeros of the Husimi distribution in the phase space.

We focused our attention at the Hamiltonian systems described by Hermitian matrices with real eigenvalues or unitary matrices with complex eigenvalues localized along the unit circle. On the other hand, there exist some recent results concerning quantum chaotic systems with dissipation [214–218]. It has been shown that under the condition of classical chaos the distribution of the eigenvalues on a complex plane displays cubic repulsion [218], typical of the Ginibre ensemble [219]. Complementary results have been obtained by an investigation of the chaotic scattering, since the poles of the scattering matrix S exhibit cubic repulsion on a complex plane [220]. Future study should be dedicated to a detailed analysis of ensembles of non–Hermitian random matrices with complex eigenvalues interpolating between universality classes, or, in the case of damped periodical systems, non-unitary matrices. Furthermore, one could attempt to apply such ensembles of random matrices to describe parametric dynamics of quantum systems with dissipation.

It is a pleasure to thank Fritz Haake for helpful remarks and warm hospitality extended to the author in Essen, where this work was started. I am grateful to Georg Lenz, Marek Kuś and Robert Serwicki for a fruitful collaboration during last three years. I have also enjoyed stimulating discussions with Barbara Dietz, Felix Izrailev, Stephen Lea, Maciej Lewenstein, Petr Šeba, Akira Shudo, Harald Wiedemann, and last but not least, Jakub Zakrzewski. Financial support from Polski Komitet Badań Naukowych, the project number 2-00799101, is gratefully acknowledged. Special thanks are due to the Alexander von Humboldt Stiftung for donating computer accessories, which facilitated the numerical calculations.

REFERENCES

[1] G. Casati, B.V. Chirikov, F.M. Izrailev, J.Ford, *Stochastic Behaviour in Classical and Quantum Hamiltonian System*, Vol. 93 of Lecture Notes in Physics, eds. G. Casati, J. Ford, Springer Verlag, Berlin 1979, p. 344.
[2] G. M. Zaslavski, *Phys. Rep.* **80**, 157 (1981).
[3] B. Eckhardt, *Phys. Rep.* **163**, 205 (1988).
[4] F. M. Izrailev, *Phys. Rep.* **196**, 299 (1990).
[5] Ya.G. Sinai, *Introduction to Ergodic Theory*, Princeton University Press, Princeton 1976.
[6] A.J. Lichtenberg, M.A. Lieberman, *Regular and Stochastic Motion*, Springer, New York, 1983.
[7] M. Toda, K. Ikeda, *Phys. Lett.* **A124**, 165 (1987).
[8] H. Frahm, H.J. Mikeska, *Z. Phys.* **B60**, 117 (1985).

[9] F. Haake, H. Wiedemann, K. Życzkowski, *Ann. Physik* **1**, 531 (1992).
[10] W.A. Majewski, M. Kuna, to appear.
[11] F. Haake, *Quantum Signatures of Chaos*, Springer, Berlin 1991.
[12] L.E. Reichl, *The Transition to Chaos*, Springer, Berlin 1992.
[13] O. Bohigas, M.J. Giannoni, C. Schmit, *Phys. Rev. Lett.* **52**, 1 (1984).
[14] T. Ishikawa, T. Yukawa, *Phys. Rev. Lett.* **54**, 1617 (1985).
[15] F. Haake, M. Kuś, R. Scharf, *Z. Phys.* **B65**, 381 (1987).
[16] C.E. Porter, *Statistical Theory of Spectra*, Academic Press, New York 1965.
[17] T.A. Brody, J. Flores, J.B. French, P.A. Mello, A. Pandey, S.S.M. Wong, *Rev. Mod. Phys.* **53**, 385 (1981).
[18] M.L. Mehta, *Random Matrices*, 2 ed., Academic Press, New York 1990.
[19] F.J. Dyson, *J. Math. Phys.* **3**, 1191 (1962).
[20] O. Bohigas, in *Chaos and Quantum Physics*, Les-Houches Session LII 1989, Eds M.J. Giannoni, A. Voros, North-Holland, Amsterdam 1991.
[21] R. Scharf, B. Dietz, M. Kuś, F. Haake, M.V. Berry, *Europhys. Lett.* **5**, 383 (1988).
[22] E.J. Heller in *Chaos and Quantum Physics*, Les-Houches Session LII 1989, Eds M.J. Giannoni, A. Voros, North-Holland, Amsterdam 1991.
[23] M.V. Berry, *Proc. R. Soc. London* **A400**, 229 (1985).
[24] M.V. Berry, *Nonlinearity*, **1**, 399 (1988).
[25] M.C. Gutzwiller, *J. Math. Phys.* **12**, 343 (1971).
[26] M.C. Gutzwiller, *Chaos in Classical and Quantum Mechanics*, Springer Verlag, Berlin 1991.
[27] D. Wintgen, *Phys. Rev. Lett.* **61**, 1803 (1988).
[28] P. Cvitanovic, B. Eckhardt, *Phys. Rev. Lett.* **63**, 823 (1989).
[29] E.B. Bogomolny, *Comm. At. Mol. Phys.* **25**, 67 (1990).
[30] A.M. Ozorio de Almeida, M. Saraceno, *Ann. Phys. (N.Y.)* **210**, 1 (1991).
[31] J.B. Keller, *Annals of Physics* **4**, 180 (1958).
[32] V.P. Maslov, *Theorie des Perturbations et Methodes Asymptotiques*, Dunod, Paris 1972.
[33] M. Sieber, F. Steiner, *Phys. Rev. Lett.* **67**, 1941 (1991).
[34] G. Tanner, P. Scherer, E.B. Bogomolny, B. Eckhardt, D. Wintgen, *Phys. Rev. Lett.* **67**, 2410 (1991).
[35] P. Dahlqvist, G. Russberg, *J. Phys. A* **24**, 4763 (1991).
[36] R. Aurich, C. Matthies, M. Sieber, F. Steiner *Phys. Rev. Lett.* **68**, 1629 (1992).
[37] S. Tomsovic, E.J. Heller, *Phys. Rev. Lett.* **67**, 665 (1991).
[38] E.A. Solovev, *Zh. Eksp. Teor. Fiz.* **82**, 1762 (1982).
[39] S. Saini, J. Zakrzewski, H.S. Taylor, *Phys. Rev.* **A38**, 3900 (1988).
[40] O. Rath, D. Richens, *J. Phys.* **B21**, 555 (1988).
[41] J. Zakrzewski, *Acta Phys. Pol.* **A77**, 745 (1990).
[42] K. Stefański, *Semiclassical Quantization of Nonintegrable Systems*, UMK Press, Toruń 1992.
[43] C. Jaffé, W.P. Reinhardt, *J. Chem. Phys.* **77**, 5191 (1982).
[44] M.V. Berry, *Physica Scripta* **40**, 335 (1989).

[45] J. Ford, in *Directions In Chaos,* Vol. II, ed. H. Bai-Lin, World Scientific, Singapore 1988.
[46] J. Bayfield, P.M. Koch, *Phys. Rev. Lett.* **33**, 258 (1974).
[47] J. Bayfield, G. Casati, I. Guarneri, D. Sokol, *Phys. Rev. Lett.* **63**, 364 (1989).
[48] R.V. Jensen, S.M. Suskind, M.M. Sanders, *Phys. Rep.*, **201**, 1 (1991).
[49] R. Blümel, U. Smilansky, *Physica Scripta* **40**, 386 (1989).
[50] G. Casati, L. Molinari, *Prog. Theor. Phys. Suppl.* **98**, 287 (1989).
[51] P.F. O'Mahony, K.T. Taylor, *Phys. Rev. Lett.* **57**, 2931 (1986).
[52] A. Holle, G. Wiebusch, J. Main, K.H. Welge, G. Zeller, G. Wunner, T. Ertl, H. Ruder, *Z. Phys.* **D5**, 279 (1987).
[53] M.L. Du, J.B. Delos, *Phys. Rev.* **A38**, 1913 (1988).
[54] D. Delande in *Chaos and Quantum Physics*, Les-Houches Session LII 1989, Eds M.J. Giannoni, A. Voros, North-Holland, Amsterdam 1991.
[55] H. Hasegawa, M. Robnik, G. Wunner, *Prog. Theor. Phys. Suppl.* **98**, 198 (1989).
[56] H. Friedrich, D. Wintgen, *Phys. Rep.* **183**, 37 (1989).
[57] *Quantum Chaos and Statistical Nuclear Physics*, Eds T.H. Seligman, H. Nishioka, Heidelberg, Springer, 1986.
[58] C.H. Lewenkopf, H.A. Weidenmüller, *Phys. Rev. Lett.* **68**, 3511 (1992).
[59] T. Ericson, *Phys. Rev. Lett.* **5**, 430 (1960).
[60] H.A. Weidenmüller, *Nucl. Phys.* **A518**, 1 (1990).
[61] B. Eckhardt, *Physica* **D33**, 89 (1988).
[62] P. Gaspard, S. Rice, *J. Chem. Phys.* **90**, 2225 (1989).
[63] R. Blümel, U. Smilansky, *Phys. Rev. Lett.* **64**, 241 (1990).
[64] J.H. Jensen, *Phys. Rev.* **A45**, 8530 (1992).
[65] S. Fishman, D.R. Grempel, R.E. Prange, *Phys. Rev. Lett.* **49**, 509 (1982).
[66] S. Fishman, *Physica Scripta* **40**, 416 (1989).
[67] D. Mailly, M. Sanquer, J-L. Pichard, P. Pari, *Europhys. Lett.* **8**, 471 (1989).
[68] Y. Imry *Europhys. Lett.* **1**, 249 (1986).
[69] S.N. Evangelou, *Phys. Rev.* **B39**, 12895 (1989).
[70] H-J. Stöckmann, J. Stein, *Phys. Rev. Lett.* **64**, 2215 (1990).
[71] S. Sridhar, *Phys. Rev. Lett.* **67**, 785, (1991).
[72] F. Haake, G. Lenz, P. Šeba, J. Stein, H-J. Stöckmann, K. Życzkowski, *Phys. Rev.* **A44**, R6161 (1991).
[73] M.V. Berry, *Ann. Phys.* **131**, 163 (1981).
[74] M.V. Berry, M. Tabor, *Proc. Roy. Soc. Lond.* **A356**, 375 (1977).
[75] A.M. Ozorio de Almeida, *Hamiltonian Systems: Chaos and Quantization,* Cambridge University Press, 1988.
[76] A.N. Kolomogorov, *Dokl. Acad. Nauk USSR* **98**, 525 (1954).
[77] V.I. Arnold, *Russian Math. Surv.* **6**, 85 (1963).
[78] J. Moser, *Math. Annalen* **169**, 3573 (1967).
[79] J.D. Meiss, *Rev. Mod. Phys.* **64**, 795 (1992).
[80] B. Chirikov, *Phys. Rep.* **52**, 263 (1979).
[81] J.M. Greene, *J. Math. Phys.* **20**, 1183 (1979).
[82] R.S. MacKay, *Physica* **7D**, 283 (1983).

[83] D.F. Escande, F. Doveil, *J. Stat. Phys.* **26**, 257 (1981).
[84] G. Hose, H.S. Taylor, *Phys. Rev. Lett.* **51**, 947 (1983).
[85] J. Bellisard, in *Lecture Notes in Math. Physics 1049*, Springer, Berlin 1985. ??
[86] R.C. Brown, R.E. Wyatt, *Phys. Rev. Lett.* **57**, 1 (1986).
[87] G. Radons, R.E. Prange, *Phys. Rev. Lett.* **61**, 1961 (1988).
[88] P. Pechukas, *Phys. Rev. Lett.* **51**, 943 (1983).
[89] T. Yukawa, *Phys. Rev. Lett.* **54**, 1883 (1985).
[90] K. Nakamura, M. Lakshmanan, *Phys. Rev. Lett.* **57**, 2772 (1986).
[91] K. Nakamura, H.J. Mikeska, *Phys. Rev.* **A35**, 5294 (1987).
[92] W.H. Steeb, A.J. van Tonder, C.M. Villet, S.J.M. Brits, *Found. Phys. Lett.* **1**, 147 (1988).
[93] J. Moser, Adv. Math. **16**, 1 (1975).
[94] S. Wojciechowski, *Phys. Lett.* **A111**, 101 (1985).
[95] B. Sutherland, *Phys. Rev.* **A5**, 1372 (1972).
[96] B. Dietz, F. Haake, *Europhysics Lett.* **9**, 1 (1989).
[97] J. Goldberg, U. Smilansky, M.V. Berry, W. Schweizer, G. Wunner, G. Zeller, *Nonlinearity*, **4**, 1 (1991).
[98] P. Gaspard, S.A. Rice, H.J. Mikeska, K. Nakamura, *Phys. Rev.* **A42**, 4015 (1990).
[99] T. Takami, *J. Phys. Soc. Jap.* **60**, 2489 (1991).
[100] D. Saher, F. Haake, P. Gaspard, *Phys. Rev.* **A44**, 7841 (1991).
[101] T. Takami, H. Hasegawa, *Phys. Rev. Lett.* **68**, 419 (1992).
[102] J. Zakrzewski, D. Delande, *Phys. Rev.* **E**, in press.
[103] M. Wilkinson, *J. Phys. A* **22**, 2795 (1989).
[104] M. Wilkinson, *Phys. Rev.* **A41**, 4645 (1990).
[105] J. Goldberg, W. Schweizer, *J. Phys. A* **24**, 2785 (1991).
[106] E.J. Austin, M. Wilkinson, *Nonlinearity* **5**, 1137 (1992).
[107] W.D. Heiss, A.L. Sannino, *J. Phys. A* **23**, 1167 (1990).
[108] J. Zakrzewski, M. Kuś, *Phys. Rev. Lett.* **67**, 2749 (1991).
[109] J. Zakrzewski, D. Delande, M. Kuś *Phys. Rev.* **E**, in press.
[110] T. Guhr, H.A. Weidenmueller, *Ann. Phys. (N.Y.)* **193**, 472 (1989).
[111] T. Guhr, H.A. Weidenmueller, *Ann. Phys. (N.Y.)* **199**, 412 (1990).
[112] T. Cheon, *Phys. Rev.* **A42**, 6227 (1990).
[113] G. Lenz, F. Haake, *Phys. Rev. Lett.* **65**, 2325 (1990).
[114] G. Lenz, K. Życzkowski, D. Saher, *Phys. Rev.* **A44**, 8043 (1991).
[115] T.H. Seligman, J.J. Verbaarschot, M.R. Zirnbauer, *J. Phys. A* **18**, 2751 (1985).
[116] G. Casati, L. Molinari, F. Izrailev, *Phys. Rev. Lett.* **64**, 1851 (1990).
[117] M. Wilkinson, M. Feingold, D.M. Leitner, *J. Phys. A* **24**, 175 (1991).
[118] G. Casati, F. Izrailev, L. Molinari, *J.Phys.* **A24**, 4755 (1991).
[119] S.N. Evangelou, E.N. Economou, *Phys. Lett.* **A151**, 345 (1990).
[120] K. Życzkowski, M. Kuś, M. Lewenstein, F. Izrailev, *Phys. Rev.* **A45**, 811 (1992).
[121] G. Casati, I. Guarneri, R. Scharf, F. Izrailev, *Phys. Rev. Lett.* **64**, 5 (1990).
[122] B. Grammaticos, A. Ramani, E. Caurier, *J. Phys. A* **23**, 5855 (1990).

[123] A. Hönig, D. Wintgen, *Phys. Rev.* **A39**, 5642 (1989).
[124] F.M. Izrailev, *Phys. Lett.* **A134**, 13 (1988).
[125] M.V. Berry, M. Robnik, *J. Phys. A* **17**, 2413 (1984).
[126] H. Hasegawa, H.J. Mikeska, H. Frahm, *Phys. Rev.* **A38**, 395 (1988).
[127] M. Robnik, *J. Phys. A* **20**, L495 (1987).
[128] H. Frahm, H.J. Mikeska, *Z. Phys.* **B65**, 249 (1986).
[129] K. Nakamura, Y. Okazaki, A.R. Bishop, *Phys. Rev. Lett.* **57**, 5 (1986).
[130] W-M. Zhang, J-M. Yuan, D.H. Feng, Q. Pan, J. Tjon, *Phys. Rev.* **A42**, 3646 (1990).
[131] P. Leboeuf, *J. Phys. A* **24**, 4575 (1991).
[132] M. Kuś, R. Scharf, F. Haake, *Z. Phys.* **B66**, 129 (1987).
[133] K. Życzkowski, G. Lenz, *Z. Phys.* **B82**, 299 (1991).
[134] G. Lenz, K. Życzkowski, *J. Phys. A* **25**, 5539 (1992).
[135] O. Bohigas, M.J. Giannoni, *Ann. Phys. (N.Y.)* **89**, 393 (1975).
[136] F. Haake, K. Życzkowski, *Phys. Rev.* **A42**, 1013 (1990).
[137] K.R.W. Jones, *J. Phys. A* **23**, L1247 (1990).
[138] J. Spanier, K.B. Oldham, *An atlas of functions*, Hemisphere Publishing Corporation, Washington 1987.
[139] *Pocketbook of Mathematical Functions*, Eds M. Abramowitz, I.A. Stegun, Harri Deutsch Verlag, Frankfurt a. Main 1984.
[140] P. Šeba, K. Życzkowski, *Phys. Rev.* **A44**, 3457 (1991).
[141] K. Życzkowski, *Acta. Phys. Pol.* **23**, 245 (1992).
[142] G. Lenz, Ph.D. thesis, Universität Essen, 1992.
[143] G. Lenz, F. Haake, *Phys. Rev. Lett.* **67**, 1 (1991).
[144] A. Pandey, M.L. Mehta, *Comm. Math. Phys.* **87**, 449 (1983).
[145] M.L. Mehta, A. Pandey, *J. Phys. A* **16**, 2622 (1983).
[146] L.D. Favro, J.F. McDonald, *Phys. Rev. Lett.* **19**, 1254 (1967).
[147] M.V. Berry, M. Robnik, *J. Phys. A* **19**, 649 (1986).
[148] R. Puri, F. Haake, to be published.
[149] B.V. Chirikov, F.M. Izrailev, D.L. Shepelyansky, *Physica* **D33**, 77 (1988).
[150] G.P. Berman, V.Yu. Rubayev, G.M. Zaslavski, *Nonlinearity* **4**, 543 (1991).
[151] A.J. Makowski, *J. Phys. A* **25**, 3419 (1992).
[152] S.T. Dembiński, A.J. Makowski, P. Pepłowski, *Phys. Rev. Lett.* **70**,1093 (1993).
[153] H.S. Camarda, *Phys. Rev.* **A45**, 597 (1992).
[154] K. Życzkowski, R. Serwicki, to appear.
[155] R. Sharf, F. Izrailev, *J. Phys. A* **23**, 963 (1990).
[156] G. Casati, I. Guarneri, F.M. Izrailev, *Phys. Lett.* **A124**, 263 (1987).
[157] Z. Cheng, J.L. Lebowitz, *Phys. Rev.* **A44**, R3399 (1991).
[158] S. Drożdż, J. Speth, *Phys. Rev. Lett.* **67**, 529 (1991).
[159] G. Casati, B.V. Chirikov, I. Guarneri, *Phys. Rev. Lett.* **54**, 1350 (1985).
[160] T.H. Seligman, J.J. Verbaarschot, *Phys. Rev. Lett.* **56**, 2767 (1986).
[161] A. Shudo, *Prog. Theor. Phys. Supll.* **98**, 173 (1989).
[162] H. Wu, M. Vallières, D.H. Feng, D.W.L. Sprung, *Phys. Rev.* **A42**, 1027 (1992).
[163] E. Yurtserver, J. Brickmann, *Phys. Rev.* **A38**, 1027 (1988).
[164] D.R. Grempel, R.E. Prange, S. Fishman, *Phys. Rev.* **A29**, 1639 (1984).

[165] M. Feingold, S. Fishman, *Physica* **D25**, 181 (1987).
[166] B.V. Chirikov, *Chaos*, **1**, 95 (1991).
[167] T. Dittrich, U. Smilansky, *Nonlinearity* **4**, 59 (1991).
[168] U. Smilansky, preprint WIS-92/15, Rehovot, 1992.
[169] B. Dietz, K. Życzkowski, *Z. Phys.* **B84**, 157 (1991).
[170] F.M. Izrailev, Phys. Lett. **125A**, 250 (1987).
[171] M. Kuś, J. Mostowski, F. Haake, *J. Phys. A* **21**, L1073 (1988).
[172] J.F. McDonald, *J. Math. Phys.* **13**, 1399 (1972).
[173] Y. Alhassid, M. Feingold, *Phys. Rev.* **A39**, 374 (1989).
[174] M. Feingold, N. Moiseyev, A. Peres, *Phys. Rev.* **A30**, 509 (1984).
[175] A. Shudo, T. Matsushita, *Phys. Rev.* **A39**, 282 (1989).
[176] M. Feingold, A. Peres, *Phys. Rev.* **A34**, 591 (1986).
[177] M. Wilkinson, *J. Phys. A* **20**, 2415 (1987).
[178] B. Eckhardt, S. Fishman, K. Müller, D. Wintgen, *Phys. Rev.* **A45**, 3531 (1992).
[179] M. Kuś, K. Życzkowski, *Phys. Rev.* **A44**, 965 (1991).
[180] K. Życzkowski, *J. Phys. A* **23**, 4427 (1990).
[181] K. Życzkowski, in *Adriatico Research Conference "Quantum Chaos", Trieste, June 1990*, p. 153, ed. H.A. Cerdeira, World Scientific, Singapore 1991.
[182] S.W. McDonald, A.N. Kaufmann, *Phys. Rev. Lett.* **42**, 1189 (1979).
[183] M. Shapiro, G. Goelman, *Phys. Rev. Lett.* **53**, 1714 (1984).
[184] S.W. McDonald, A.N. Kaufmann, *Phys. Rev.* **A37**, 3067 (1988).
[185] E. Heller, *Phys. Rev. Lett.* **53**, 1515 (1984).
[186] E.B. Bogomolny, *Physica* **D31**, 169 (1988).
[187] M.V. Berry, *Proc. Roy. Soc. (London)* **A423**, 219 (1989).
[188] E.J. Heller, P.W. O'Connor, J. Gehlen, *Physica Scripta* **40**, 354 (1989).
[189] M. Feingold, R.G. Littlejohn, S.B. Solina, J.S. Pehling, O. Piro, *Phys. Lett.* **A146**, 199 (1990).
[190] R. Aurich, F. Steiner, *Physica* **D48**, 445 (1991).
[191] G.M. D'Ariano, L.R. Evangelista, M. Saraceno, *Phys. Rev.* **A45**, 3646 (1992).
[192] D.C. Meredith, *J. Stat. Phys.* **68**, 97 (1992).
[193] G. Chu, J.V. José, *J. Stat. Phys.* **68**, 153 (1992).
[194] M. Kuś, J. Zakrzewski, K. Życzkowski, *Phys. Rev.* **A43**, 4244, (1991).
[195] J. Gibbson, T. Hermsen, S. Wojciechowski, *Phys. Lett.* **A94**, 251 (1983).
[196] M.A. Olshanetzky, A.M. Perelomov, *Phys. Rep.* **71**, 313, (1981).
[197] M. Kuś, *Europhys. Lett.* **5**, 1 (1988).
[198] R. Sharf, M. Kuś, *Phys. Rev.* **A40**, 4774 (1989).
[199] D. Saher, *Z. Phys.* **B85**, 105 (1991).
[200] F.M. Izrailev, D.L. Shepelyanski, *Dokl. Akad. Nauk. SSSR* **249**, 1103 (1979).
[201] T. Hogg, B.A. Huberman, *Phys. Rev.* **A28**, 22 (1983).
[202] G. Casati, I. Guarneri, *Comm. Math. Phys.* **95**, 121 (1984).
[203] K. Nakamura, A.R. Bishop, A. Shudo, *Phys. Rev.* **B39**, 12422 (1989).
[204] F. Haake, D.L. Shepelyansky, *Europhys. Lett.* **5**, 671 (1988).
[205] A. Peres, in *Adriatico Research Conference "Quantum Chaos", Trieste, June 1990*, ed. H.A. Cerdeira, World Scientific, Singapore 1991.

[206] E. Bogomolny, O. Bohigas, P. Leboeuf, *Phys. Rev. Lett.* **68**, 2726 (1992).
[207] K. Nakamura, *Prog. Theor. Phys. Suppl.* **98**, 383 (1989).
[208] H.G. Schuster, *Deterministic Chaos*, Verlags, Meinheim 1988.
[209] G. Benettin, L. Galgani, J-M. Strielcyn, *Phys. Rev.* **A14**, 2338 (1976).
[210] W.A. Lin, L.E. Reichl, *Phys. Rev.* **A40**, 1055 (1989).
[211] B. Dietz, F. Haake, *Z. Phys.* **B80**, 153 (1990).
[212] M. Toda, *Physica* **D59**, 121 (1992).
[213] M.B. Cibils, Y. Cuche, P. Leboeuf, W.F. Wreszinski, *Phys. Rev.* **A46**, 4560 (1992).
[214] R. Grobe F. Haake, *Z. Phys.* **B68**, 503 (1987).
[215] P. Pepłowski, S.T. Dembiński, *Z. Phys.* **B83**, 453 (1991).
[216] T. Diettrich, R. Graham, *Z. Phys.* **B62**, 515 (1986).
[217] T. Diettrich, R. Graham, *Europhys. Lett.* **7**, 287 (1988).
[218] R. Grobe, F. Haake, *Phys. Rev. Lett.* **62**, 2893 (1989).
[219] J. Ginibre, *J. Math. Phys. (N.Y.)* **6**, 440 (1965).
[220] W. John, B. Milek, H. Schanz, P. Šeba, *Phys. Rev. Lett.* **67**, 1949 (1991).